The Astronomical Journal, 155:265 (23pp), 2018 June https://doi.org/10.3847/1538-3881/aac262


# The Solar Neighborhood XLIV: RECONS Discoveries within 10 parsecs

Todd J. Henry[1,8], Wei-Chun Jao[2,8], Jennifer G. Winters[3,8], Sergio B. Dieterich[4,8], Charlie T. Finch[5,8], Philip A. Ianna[1,8], Adric R. Riedel[6,8], Michele L. Silverstein[2,8], John P. Subasavage[7,8], and Eliot Halley Vrijmoet[2]
[1] RECONS Institute, Chambersburg, PA 17201, USA; toddhenry28@gmail.com, philianna3@gmail.com
[2] Department of Physics and Astronomy, Georgia State University, Atlanta, GA 30302, USA; jao@astro.gsu.edu, silverstein@astro.gsu.edu, vrijmoet@astro.gsu.edu
[3] Harvard-Smithsonian Center for Astrophysics, Cambridge, MA 02138, USA; jennifer.winters@cfa.harvard.edu
[4] Department of Terrestrial Magnetism, Carnegie Institution for Science, Washington, DC 20015, USA; sdieterich@carnegiescience.edu
[5] Astrometry Department, U.S. Naval Observatory, Washington, DC 20392, USA; charlie.finch@navy.mil
[6] Space Telescope Science Institute, Baltimore, MD 21218, USA; adric.riedel@gmail.com
[7] United States Naval Observatory, Flagstaff, AZ 86001, USA; jsubasavage@nofs.navy.mil
*Received 2018 April 12; revised 2018 April 27; accepted 2018 May 1; published 2018 June 4*

## Abstract

We describe the 44 systems discovered to be within 10 pc of the Sun by the RECONS team, primarily via the long-term astrometry program at the CTIO/SMARTS 0.9 m that began in 1999. The systems—including 41 with red dwarf primaries, 2 white dwarfs, and 1 brown dwarf—have trigonometric parallaxes greater than 100 mas, with errors of 0.4–2.4 mas in all but one case. We provide updated astrometric, photometric (*VRIJHK* magnitudes), spectral type, and multiplicity information here. Among these are 14 systems that are new entries to the 10 pc sample, including the first parallaxes for 9 systems and new values for 5 systems that had previous parallaxes with errors greater than 10 mas or values placing them beyond 10 pc. We also provide new data for 22 systems known to lie within 10 pc and 9 systems reported to be closer than that horizon but for which new parallaxes place them further away, bringing the total to 75 systems. The 44 systems added by RECONS comprise one of every 7 systems known within 10 pc. We illustrate the evolution of the 10 pc sample from the 191 systems known when the final Yale Parallax Catalog was published in 1995 to the 317 systems known today. Even so close to the Sun, additional discoveries of white, red, and brown dwarfs are possible, both as primaries and secondaries, although we estimate that at least 90% of the stellar systems closer than 10 pc have now been identified.

*Key words:* astrometry – solar neighborhood – stars: distances – stars: low-mass – stars: statistics – surveys

*Supporting material:* machine-readable tables

## 1. Introduction

The solar neighborhood holds a special place in the human psyche, because by our very nature, humans explore the nearest locales first. Space is no exception. The nearest stars provide the framework upon which stellar astrophysics is based because the nearby star population contains the most easily studied representatives of their kinds. So, it is essential that we make a careful reconnaissance of the nearest stars to understand our Sun and Solar System in context.

The REsearch Consortium On Nearby Stars (RECONS, www.recons.org) was established in 1994 to discover "missing" members of the solar neighborhood and to characterize the complete sample of nearby star systems and their environs. Over the past two decades, we have published RECONS results in papers in this series, *The Solar Neighborhood*, in *The Astronomical Journal*. This paper focuses on the 10 pc sample, in which a system composed of stars, brown dwarfs, and/or planets is included if a trigonometric parallax, $\pi_{trig}$, of at least 100 mas has been determined, and the parallax has a formal error, $\sigma_\pi$, of 10 mas or less. Here we report trigonometric parallaxes measured at the Cerro Tololo Inter-American Observatory (CTIO)/Small and Moderate Aperture Research Telescope System (SMARTS) 0.9 m for 14 systems that are new additions to the 10 pc sample,[9] as well as for 30 other systems discovered by RECONS to be within 10 pc. We also outline the growth of the 10 pc sample since the 1995 publication of the largest ground-based compendium, *The General Catalogue of Trigonometric Stellar Parallaxes* (van Altena et al. 1995), also known as the "Yale Parallax Catalog" (hereafter YPC). We include the contributions by the space-based *Hipparcos* effort (ESA 1997; Perryman et al. 1997), with initial results published in 1997, and utilize the updated parallaxes from the van Leeuwen (2007) reduction done a decade later; for stars within 10 pc, there are no significant differences that change the sample membership. The new results and overview presented here set the stage for the full analysis of the 10 pc sample to be evaluated after parallaxes are available from *Gaia* in Data Release 2.

We outline the observing program and target sample in Section 2, followed by a description of the observations in Section 3. Astrometric, photometric, and spectroscopic results for all 75 systems in this study, including the 44 added by RECONS to the 10 pc sample, are given in Section 4. Systems worthy of note are described in Section 5. Finally, the evolution of the 10 pc sample since 1995 and the contributions made by RECONS and others are placed in context in Section 6.

## 2. Observing Program and Sample

A primary goal of the RECONS effort has been to discover and characterize white, red, and brown dwarfs in the southern sky within 25 pc. To this end, the RECONS team began a parallax program at CTIO in 1999 under the auspices of the NOAO Surveys Program, using both the 0.9 m and 1.5 m

[8] Visiting Astronomer, Cerro Tololo Inter-American Observatory. CTIO is operated by AURA, Inc., under contract to the National Science Foundation.
[9] We also provide parallaxes from URAT confirming that seven of the new systems are within 10 pc.

CTIO/SMARTS telescopes. Optical photometry was also obtained at both telescopes, and spectra were obtained at the 1.5 m and CTIO 4.0 m. Parallaxes for a total of 58 systems with $VRI = 11$–23 were measured at the 1.5 m and published in Costa et al. (2005, 2006). The 0.9 m effort has continued to the present as an expanded astrometry/photometry program via the SMARTS Consortium, which was formed in 2003. More than 800 systems with $VRI = 9$–18 have been observed for parallax at the 0.9 m, with new results presented here in Section 4.

The objects targeted in the RECONS program at CTIO fall into two general categories: those that have high proper motions or crude trigonometric parallaxes indicating they might be nearby, and those with optical/infrared photometry or spectroscopy hinting that they might be closer than 25 pc. Systems with declinations south of $+30°$ have been observed astrometrically, photometrically, and spectroscopically to pinpoint their distances, proper motions, absolute magnitudes, colors, and spectral types. By providing this full suite of data, well-characterized new members can be added to the 25 pc sample. In this paper we collect and update results for the full set of 44 new systems found within 10 pc via this effort, provide new results for 22 previously identified 10 pc systems, and add results for 9 additional systems that were previously reported to be within 10 pc for which our parallaxes place them beyond that horizon. In total, we present information for 75 systems composed of primarily red dwarfs, with a few white and brown dwarfs as well.

## 3. Observations

### 3.1. Astrometry

A single camera, equipped with a Tektronics 2048 × 2046 CCD having pixels 401 mas square on the sky, has been used at the 0.9 m since 1999. The nearby systems described here were observed for 2.0–18.4 years (median coverage 13.1 years) in an effort to reach parallax precisions of 3 mas or better, corresponding to distances accurate to 3% at 10 pc. Both astrometry and photometry observations (the latter discussed in Section 3.2) utilize only the central quarter of the CCD ($6\farcm8 \times 6\farcm8$ field of view), primarily to minimize astrometric distortions. For the astrometric observations, targets are observed through one of three *VRI* filters,[10] except for a period from 2005 March through 2009 June, when the cracked Tek #2 *V* filter was temporarily replaced by the very similar Tek #1 *V* filter. Reductions indicate no significant differences in photometric results from the two *V* filters, although astrometric offsets are seen, as described in Subasavage et al. (2009) and Riedel et al. (2010). When possible, these astrometric offsets are minimized by choosing reference stars very close to the targets.

A target's parallax and proper motion are usually considered worthy of publication when ∼12 visits of ∼5 frames each are collected on different nights spread over at least two years, typically resulting in parallaxes with errors of ∼1.5 mas and proper motions with errors $<1$ mas yr$^{-1}$. The 75 systems described here have parallax errors of 0.48–2.37 mas (median value 1.02 mas), except for DEN 0255-4700 (error 3.98 mas), which was only observed at the 1.5 m. Thus, the resulting distances are known to ∼2% or better.

As this is the 20th paper to report parallaxes from the 0.9 m,[11] we provide only brief information on the observing techniques and data reduction here; additional details can be found in previous papers in this series, particularly in Jao et al. (2005) and Henry et al. (2006). Data are reduced via IRAF with typical bias subtraction and dome flat-fielding, using calibration frames taken at the beginning of each night. The frames are then analyzed using our astrometric pipeline, utilizing images taken within 120 minutes of transit to produce parallaxes, proper motions, and time-series photometry in the parallax filter (see Section 4.2). Target positions are measured relative to 5–19 reference stars within a few arcminutes of the targets, resulting in relative trigonometric parallaxes and proper motions. Parallaxes are corrected from relative to absolute values using the mean of the photometric distances to the reference stars. For a few targets, the distant reference stars appear reddened and result in corrections of 3 mas or more. In these cases we adopt our typical correction of $1.50 \pm 0.50$ mas for 0.9 m observations. This value is in the midst of the range of corrections for other stars in this sample (0.28–2.76 mas) and provides for a generous uncertainty (only three systems have larger correction uncertainties), which is appropriate given that we have estimated the correction.

We also report parallaxes from the United States Naval Observatory Robotic Astrometric Telescope (URAT) in the notes for seven systems (Section 5) that support our RECONS measurements placing these systems within 10 pc. URAT observations were taken at CTIO over a 2-year period that overlapped with the long-term work described for the RECONS effort, and details of the southern portion of the URAT program can be found in Finch et al. (2018). Although the URAT parallax errors of 3.4–5.6 mas for these seven systems are larger than for the RECONS measurements, having two parallaxes that place systems within 10 pc provides valuable confirmation.

### 3.2. Photometry

Optical *VRI* photometry was acquired at the 0.9 m using the same camera/filter/detector combination used for the astrometry frames, as described in Section 3.1. A modicum of additional photometry was acquired at the SOAR 4.1 m and CTIO/SMARTS 1.0 m as part of other RECONS programs (in particular, see Dieterich et al. 2014 and Winters et al. 2011 for details). All photometry is on the Johnson–Kron–Cousins (JKC) system, determined using photometric standards taken nightly to derive transformation equations and extinction curves, primarily from Landolt (1992), supplemented with standards from Bessell (1990), Graham (1982), and Landolt (2007, 2013). These standard star sets were augmented with a few of our own red standards—GJ 1061, LHS 1723, LHS 2090, SCR 1845-6357 AB, and SO 0253+1652—for which standard *VRI* magnitudes are included in Table 3. The SOAR photometry was taken using a Bessell filter set, but has been converted to the JKC system as described in Dieterich et al. (2014).

Photometric apertures 14″ in diameter were typically used to determine the stellar fluxes to match the apertures used by Landolt. Smaller apertures were used and aperture corrections done when targets were corrupted by nearby sources such as physical companions or background objects, or for very faint

[10] The central wavelengths for $V_J$, $R_{KC}$, and $I_{KC}$ are 5475 Å, 6425 Å, and 8075 Å, respectively, hereafter without the subscripts J = Johnson and KC = Kron–Cousins.

[11] The full library of papers can be found at http://www.recons.org.

sources in an effort to reduce the contribution of the sky background. Typical errors in the *VRI* values are 0.03 mag because longer exposure times are used for fainter targets, as discussed in Henry et al. (2004) and Winters et al. (2011).

### 3.3. Spectroscopy

Spectra were obtained for nearby star candidates between 1995 and 2011 using the CTIO 1.5 m and 4.0 m telescopes. We have previously reported spectroscopy techniques and results in various papers in this series (Henry et al. 2002, 2004, 2006; Jao et al. 2008, 2011; Riedel et al. 2011, 2014; Lurie et al. 2014). Briefly, the 1.5 m data were taken using a 2.″0 slit in the RC Spectrograph with grating #32 in first order and order blocking filter OG570 to provide wavelength coverage from 6000 to 9500 Å and resolution of 8.6 Å on the Loral 1200 × 800 CCD. At the 4.0 m, data were taken using a 2.″0 slit in the RC Spectrograph with grating G181 and order blocking filter OG515 to provide wavelength coverage from 5000 to 10700 Å and resolution of 5.6 Å on the Loral 3K×1K CCD. Typically, two sequential exposures were taken of a star to permit cosmic ray removal. Additional details of the observational setups and data reduction can be found in Henry et al. (2002) and Jao et al. (2008).

Spectral types for many of the red dwarfs in the sample have been reported in previous papers in this series. We provide new spectral types here, updated following the methodology described in Riedel et al. (2014). Both the 1.5 m and 4.0 m data were reduced with standard IRAF techniques using calibration frames of several flux standards taken during each observing run. Mild fringing in the 4.0 m data caused by back illumination of the CCD was removed with a tailored IDL routine. After extraction, each spectrum was normalized at 7500 Å, interpolated in 1 Å intervals from 6000 to 9000 Å, and best matches were found between the measured flux pairs for each target and standard. Telluric lines were not removed, so wavelengths in telluric bands, as well as the region around the variable H$\alpha$ line, were omitted during matching. The best spectral type was selected using the lowest standard deviation value, measured using $\mathrm{stddev}\left(\frac{\mathrm{target}}{\mathrm{standard}}\right)$. The resulting spectral types for the M dwarfs in this study have uncertainties of 0.5 subtypes.

The spectral types given here supersede those in previous papers (e.g., types in Henry et al. 1994, 2002, 2006), because the spectra have been reanalyzed on the new system and consequent adjustments to types have been made. Comparisons to spectral types from the large RHG survey of M stars reported in Reid et al. (1995) and Hawley et al. (1996) indicate that the types are consistent to ∼0.5 subtypes, with RECONS types being slightly earlier in some cases.

## 4. Results

### 4.1. Astrometry

Astrometry results are given in Table 1, with names in columns (1–2), followed R.A. and decl. 2000.0 positions (3–4). The next column lists the discovery reference that added the system to the 10 pc sample via $\pi_{\mathrm{trig}}$ (5), and in cases of updates by us, we provide the duration of the astrometric series at the time (6). Specifics of the observations are listed next, including the filter used (7); the number of seasons (8), where "c" indicates continuous coverage and "s" indicates scattered coverage in at least some seasons; the number of frames (9), the dates (10) and durations (11) of the series; and the number of reference stars used in the reductions (12). Measured relative trigonometric parallaxes ($\pi$ (rel), 13), corrections to absolute parallaxes (14),[12] and absolute parallaxes ($\pi$ (abs), 15) are given next, followed by relative proper motion magnitudes ($\mu$, 16) and position angles ($\theta$, north through east, 17), and derived tangential velocities ($V_{\mathrm{tan}}$, 18) using the measured results. In the final column (19) we provide brief notes.

The top portion of Table 1 lists the 44 systems that the RECONS effort has placed within 10 pc, with the proviso that the $\pi_{\mathrm{trig}}$ error must be less than 10 mas. These 44 systems include 30 previously published (most parallaxes updated here) and 14 new systems, indicated with "new" in column (5). The 14 new systems added to the 10 pc sample include nine singles and five doubles. In the middle portion of Table 1 we list parallaxes for 22 additional important systems known to be within 10 pc. We have observed most of these for many years and in some cases confirm parallaxes recently reported to be larger than 100 mas by other groups, whereas for other targets we provide updates that differ by 5 mas or more from previously available values. Finally, the lower portion of Table 1 includes nine systems that were reported to be within 10 pc, but our new parallaxes place them beyond that horizon, including LP 647-013, LHS 1302, and APM 0237-5928 that we previously had just within 10 pc. These are to be contrasted with GJ 203 and GJ 595 AB, two systems that were beyond 10 pc, but we pull into the sample with new parallax measurements. Noteworthy astrometric results for individual systems are discussed in Section 5.

Of the 44 systems added to the 10 pc sample, six are within 5 pc, including the closest, GJ 1061 (3.7 pc), that we first reported in Henry et al. (1994). Six of the systems within 10 pc were discovered during our SuperCOSMOS-RECONS (SCR) survey: SCR 0740-4257 (7.8 pc), SCR 1546-5534 AB (9.7 pc), and SCR 2049-4012 AB (9.6 pc) have parallaxes reported here for the first time, and we provide updated measurements for SCR 0630-7643 AB (8.8 pc), SCR 1138-7721 (8.4 pc), and SCR 1845-6357 AB (4.0 pc), all first reported in Henry et al. (2006). The 44 systems have proper motions ranging from 68 to 5103 mas yr$^{-1}$, with 14 moving faster than 1.″0 yr$^{-1}$. Among these are four of the five systems with the slowest proper motions within 10 pc: SCR 2049-4012 AB (68 mas yr$^{-1}$), WIS 0720-0846 AB (109 mas yr$^{-1}$), L 173-019 (126 mas yr$^{-1}$), and UPM 0815-2344 AB (138 mas yr$^{-1}$).

Figure 1 illustrates LHS 2090 as an example of a single star with no detected companions, and five systems (shown alphabetically by name) exhibiting perturbations with full orbits covered in the astrometric data. The photocentric positions for each target have been separated into two panels, split into R.A. and decl. components, and the points represent positions after shifts due to proper motion and parallax have been removed. Shown for the five systems are orbital fits with periods of 0.17–6.74 years that have been derived using the fitting protocol of Hartkopf et al. (1989). All orbital fits have been made using only the astrometry data. The parallaxes given in Table 1 are those derived once the perturbations have been removed. In Table 2, we provide photocentric orbital elements

[12] In four cases, generic corrections of 1.50 ± 0.50 mas have been used to adjust from relative to absolute parallaxes, as noted in the final column of Table 1. This generic correction is used when the reference stars are significantly reddened, resulting in erroneous distance estimates for stars comprising the reference field.

**Table 1**
Astrometric Results

| Name (1) | Other Name (2) | R.A. J2000.0 (3) | Decl. J2000.0 (4) | Disc. Ref. (5) | Time years (6) | Filter (7) | $N_{sea}$ (8) | $N_{frm}$ (9) | Coverage (10) | Time years (11) | $N_{ref}$ (12) | $\pi$(rel) mas (13) | $\pi$(corr) mas (14) | $\pi$(abs) mas (15) | $\mu$ mas yr$^{-1}$ (16) | $\theta$ degree (17) | $V_{tan}$ km s$^{-1}$ (18) | Notes (19) |
|---|---|---|---|---|---|---|---|---|---|---|---|---|---|---|---|---|---|---|
| New 10 pc Members—44 Systems | | | | | | | | | | | | | | | | | | |
| GJ 2005 ABC | LHS 1070 ABC | 00 24 44.19 | −27 08 24.2 | Cos05 | 2.30 | *R* | 19s | 172 | 1999.64 −2017.93 | 18.30 | 6 | 138.32 ± 1.59 | 0.98 ± 0.04 | 139.30 ± 1.59 | 687.3 ± 0.3 | 350.5 ± 0.04 | 23.4 | orbit fit |
| WD 0038-226 | GJ 2012 | 00 41 26.03 | −22 21 02.3 | Sub09 | 8.25 | *R* | 18s | 168 | 1999.64 −2016.97 | 17.33 | 7 | 109.60 ± 0.76 | 1.24 ± 0.07 | 110.84 ± 0.76 | 608.2 ± 0.1 | 232.6 ± 0.02 | 26.0 | |
| WD 0141-675 | LHS 145 | 01 43 00.98 | −67 18 30.4 | Sub09 | 7.42 | *V* | 12s | 163 | 2000.57 −2015.82 | 15.25 | 6 | 100.92 ± 0.79 | 0.88 ± 0.07 | 101.80 ± 0.79 | 1079.6 ± 0.2 | 199.2 ± 0.01 | 50.3 | Sub17 result |
| L 173-019 | | 02 00 38.31 | −55 58 04.8 | new | … | *V* | 9s | 120 | 2007.81 −2015.97 | 8.16 | 7 | 122.77 ± 2.07 | 0.34 ± 0.18 | 123.11 ± 2.08 | 125.5 ± 0.8 | 123.5 ± 0.74 | 4.8 | |
| SO 0253+1652 | | 02 53 00.89 | +16 52 52.7 | Hen06 | 2.35 | *I* | 13s | 165 | 2003.53 −2015.83 | 12.30 | 6 | 258.25 ± 1.73 | 2.76 ± 0.32 | 261.01 ± 1.76 | 5103.1 ± 0.5 | 138.1 ± 0.01 | 92.7 | |
| DENIS 0255-4700 | | 02 55 03.68 | −47 00 51.6 | Cos06 | 3.20 | *I* | … | 44 | … | 3.20 | 17 | 201.14 ± 3.89 | 0.23 ± 0.05 | 201.37 ± 3.89 | 1148.5 ± 2.2 | 119.5 ± 0.21 | 27.0 | Cos06 result (1.5 m) |
| LTT 1445 A | LP 771-095 | 03 01 51.04 | −16 35 31.0 | Hen06 | 6.33 | *V* | 16s | 234 | 1999.64 −2017.80 | 18.17 | 5 | 142.90 ± 1.58 | 0.95 ± 0.14 | 143.85 ± 1.59 | 480.7 ± 0.3 | 234.9 ± 0.06 | 15.8 | orbit fit |
| LTT 1445 BC | LP 771-096 AB | 03 01 51.04 | −16 35 31.0 | Hen06 | 6.15 | *V* | 16s | 234 | 1999.64 −2017.80 | 18.17 | 5 | 141.62 ± 2.03 | 0.95 ± 0.14 | 142.57 ± 2.03 | 479.4 ± 0.3 | 234.1 ± 0.08 | 15.9 | orbit fit |
| GJ 1061 | LHS 1565 | 03 35 59.72 | −44 30 45.5 | Hen97 | 6.33 | *R* | 17s | 255 | 1999.62 −2016.04 | 16.42 | 7 | 269.59 ± 1.18 | 0.94 ± 0.08 | 270.53 ± 1.18 | 827.3 ± 0.2 | 118.1 ± 0.03 | 14.5 | |
| LHS 1610 AB | | 03 52 41.76 | +17 01 04.3 | Hen06 | 6.25 | *V* | 15s | 175 | 1999.71 −2014.94 | 15.23 | 7 | 104.14 ± 1.65 | 1.45 ± 0.23 | 105.59 ± 1.67 | 767.1 ± 0.3 | 146.2 ± 0.05 | 34.4 | |
| GJ 1068 | LHS 22 | 04 10 28.14 | −53 36 08.2 | Jao05 | 3.96 | *R* | 19s | 266 | 1999.64 −2018.07 | 18.43 | 5 | 142.03 ± 0.70 | 1.88 ± 0.12 | 143.91 ± 0.71 | 2562.5 ± 0.2 | 199.5 ± 0.01 | 84.4 | |
| LHS 1723 | | 05 01 57.43 | −06 56 46.5 | Hen06 | 6.14 | *V* | 16s | 279 | 1999.81 −2014.93 | 15.12 | 8 | 184.72 ± 0.73 | 1.47 ± 0.21 | 186.19 ± 0.76 | 772.6 ± 0.2 | 226.3 ± 0.03 | 19.7 | |
| LTT 17736 | G 097-015 | 05 04 14.76 | +11 03 23.8 | new | … | *R* | 12s | 138 | 2006.07 −2016.05 | 9.98 | 8 | 99.49 ± 0.90 | 1.50 ± 0.50 | 100.99 ± 1.03 | 206.6 ± 0.2 | 342.6 ± 0.12 | 9.7 | generic $\pi_{corr}$ |
| GJ 203 | ROSS 41 | 05 28 00.15 | +09 38 38.2 | new | … | *V* | 7s | 75 | 2009.94 −2015.96 | 6.03 | 9 | 102.45 ± 1.48 | 2.31 ± 0.34 | 104.76 ± 1.52 | 777.6 ± 0.7 | 194.7 ± 0.08 | 35.2 | |
| LTT 17897 | G 099-049 | 06 00 03.52 | +02 42 23.6 | Hen06 | 6.06 | *V* | 16s | 397 | 1999.91 −2014.93 | 15.02 | 6 | 191.73 ± 1.01 | 2.52 ± 1.57 | 194.25 ± 1.87 | 308.3 ± 0.3 | 097.3 ± 0.09 | 7.5 | |
| AP COL | | 06 04 52.16 | −34 33 36.0 | Rie11 | 6.48 | *V* | 14c | 248 | 2004.91 −2018.07 | 13.16 | 14 | 115.45 ± 0.80 | 0.96 ± 0.10 | 116.41 ± 0.81 | 342.1 ± 0.2 | 004.3 ± 0.05 | 13.9 | |
| SCR 0630-7643 AB | | 06 30 46.61 | −76 43 08.9 | Hen06 | 2.03 | *I* | 13s | 114 | 2003.96 −2017.08 | 13.12 | 8 | 112.02 ± 1.43 | 2.09 ± 0.19 | 114.11 ± 1.44 | 461.8 ± 0.4 | 356.9 ± 0.07 | 19.2 | |
| WIS 0720-0846 AB | | 07 20 03.25 | −08 46 50.0 | new | … | *I* | 5c | 109 | 2013.92 −2017.91 | 3.99 | 11 | 147.75 ± 1.07 | 1.05 ± 0.14 | 148.80 ± 1.08 | 109.3 ± 0.9 | 208.8 ± 0.86 | 3.5 | orbit fit |
| LTT 17993 AB | G 089-032 AB | 07 36 25.13 | +07 04 43.1 | Hen06 | 6.05 | *R* | 19s | 297 | 1999.91 −2017.94 | 18.03 | 13 | 116.66 ± 0.83 | 0.93 ± 0.08 | 117.59 ± 0.83 | 390.7 ± 0.1 | 142.8 ± 0.04 | 15.7 | orbit fit |
| SCR 0740-4257 | | 07 40 11.80 | −42 57 40.3 | new | … | *R* | 12c | 201 | 2004.97 −2016.05 | 11.08 | 12 | 126.10 ± 0.73 | 1.61 ± 0.22 | 127.71 ± 0.76 | 695.0 ± 0.2 | 316.6 ± 0.03 | 25.8 | |
| GJ 300 | LHS 1989 | 08 12 40.88 | −21 33 06.8 | Hen06 | 6.05 | *V* | 16s | 258 | 1999.91 −2014.95 | 15.04 | 8 | 121.51 ± 0.40 | 1.27 ± 0.26 | 122.78 ± 0.48 | 698.6 ± 0.1 | 178.6 ± 0.01 | 27.0 | |
| UPM 0815-2344 AB | | 08 15 11.19 | −23 44 15.7 | new | … | *V* | 4c | 87 | 2014.92 −2018.15 | 3.24 | 10 | 103.84 ± 0.86 | 1.21 ± 0.11 | 105.05 ± 0.87 | 137.8 ± 0.7 | 062.6 ± 0.57 | 6.2 | |
| L 098-059 | | 08 18 07.63 | −68 18 46.9 | new | … | *R* | 11s | 130 | 2006.21 −2016.06 | 9.86 | 9 | 99.67 ± 2.35 | 2.14 ± 0.27 | 101.81 ± 2.37 | 365.1 ± 0.8 | 165.2 ± 0.23 | 17.0 | |
| LTT 12352 ABC | G 041-014 ABC | 08 58 56.33 | +08 28 26.0 | Hen06 | 5.99 | *V* | 19s | 255 | 1999.97 −2017.94 | 17.97 | 5 | 145.24 ± 1.50 | 1.73 ± 0.16 | 146.97 ± 1.51 | 502.8 ± 0.2 | 130.5 ± 0.05 | 16.2 | |
| LHS 2090 | | 09 00 23.55 | +21 50 04.8 | Hen06 | 2.92 | *I* | 15s | 168 | 2002.28 −2016.06 | 13.78 | 7 | 155.57 ± 1.06 | 1.75 ± 0.22 | 157.32 ± 1.08 | 774.9 ± 0.2 | 221.2 ± 0.03 | 23.3 | |
| LHS 6167 AB | | 09 15 36.40 | −10 35 47.2 | Bar17 | 9.31 | *V* | 14s | 156 | 2003.94 −2017.21 | 13.27 | 7 | 102.46 ± 0.75 | 1.08 ± 0.18 | 103.54 ± 0.77 | 439.4 ± 0.2 | 244.3 ± 0.04 | 20.1 | orbit fit |
| GJ 1123 | LHS 263 | 09 17 05.33 | −77 49 23.4 | Jao05 | 4.10 | *V* | 13s | 142 | 2002.23 −2018.07 | 15.85 | 13 | 103.01 ± 1.13 | 1.53 ± 0.26 | 104.54 ± 1.16 | 1040.2 ± 0.3 | 141.5 ± 0.03 | 47.2 | |
| GJ 1128 | LHS 271 | 09 42 46.36 | −68 53 06.1 | Jao05 | 4.10 | *V* | 17s | 217 | 2000.23 −2017.08 | 16.85 | 8 | 154.02 ± 0.69 | 0.73 ± 0.11 | 154.75 ± 0.70 | 1123.0 ± 0.1 | 356.1 ± 0.01 | 34.4 | |

**Table 1**
(Continued)

| Name (1) | Other Name (2) | R.A. J2000.0 (3) | Decl. J2000.0 (4) | Disc. Ref. (5) | Time years (6) | Filter (7) | $N_{sea}$ (8) | $N_{frm}$ (9) | Coverage (10) | Time years (11) | $N_{ref}$ (12) | $\pi$(rel) mas (13) | $\pi$(corr) mas (14) | $\pi$(abs) mas (15) | $\mu$ mas yr$^{-1}$ (16) | $\theta$ degree (17) | $V_{tan}$ km s$^{-1}$ (18) | Notes (19) |
|---|---|---|---|---|---|---|---|---|---|---|---|---|---|---|---|---|---|---|
| LHS 2206 | | 09 53 55.19 | +20 56 46.8 | Hen06 | 5.91 | *R* | 16s | 178 | 2000.06 −2015.07 | 15.01 | 6 | 108.94 ± 1.80 | 0.91 ± 0.05 | 109.85 ± 1.80 | 520.5 ± 0.3 | 319.0 ± 0.07 | 22.5 | |
| LHS 288 | | 10 44 21.24 | −61 12 35.6 | Hen06 | 5.07 | *R* | 18s | 200 | 2000.06 −2017.18 | 17.12 | 10 | 208.41 ± 0.81 | 1.04 ± 0.14 | 209.45 ± 0.82 | 1643.9 ± 0.2 | 348.2 ± 0.01 | 37.2 | |
| DENIS 1048-3956 | | 10 48 14.56 | −39 56 07.0 | Jao05 | 3.18 | *I* | 16s | 216 | 2001.15 −2016.05 | 14.90 | 11 | 246.93 ± 0.59 | 0.85 ± 0.10 | 247.78 ± 0.60 | 1532.0 ± 0.1 | 229.9 ± 0.01 | 29.3 | |
| SCR 1138-7721 | | 11 38 16.76 | −77 21 48.5 | Hen06 | 2.09 | *I* | 15s | 171 | 2003.25 −2017.19 | 13.94 | 12 | 118.92 ± 0.92 | 0.81 ± 0.07 | 119.73 ± 0.92 | 2143.0 ± 0.2 | 286.9 ± 0.01 | 84.8 | |
| SIPS 1141-3624 | | 11 41 21.52 | −36 24 34.7 | new | … | *R* | 10s | 110 | 2007.31 −2016.05 | 8.74 | 12 | 114.66 ± 1.29 | 1.46 ± 0.14 | 116.12 ± 1.30 | 579.4 ± 0.5 | 057.4 ± 0.10 | 23.7 | |
| LHS 337 | | 12 38 49.10 | −38 22 53.8 | Hen06 | 3.19 | *R* | 14s | 142 | 2002.28 −2017.20 | 14.92 | 14 | 149.27 ± 1.02 | 1.41 ± 0.14 | 150.68 ± 1.03 | 1463.1 ± 0.2 | 206.4 ± 0.02 | 46.0 | |
| WT 460 AB | | 14 11 59.93 | −41 32 21.3 | Hen06 | 5.43 | *I* | 18s | 317 | 2000.14 −2017.47 | 17.33 | 11 | 106.70 ± 0.73 | 1.83 ± 0.13 | 108.53 ± 0.74 | 734.6 ± 0.2 | 261.3 ± 0.02 | 32.1 | orbit fit |
| WIS 1540-5101 | | 15 40 43.52 | −51 01 35.9 | new | … | *R* | 3s | 48 | 2014.45 −2016.46 | 2.00 | 10 | 186.46 ± 1.09 | 1.47 ± 0.38 | 187.93 ± 1.15 | 1981.2 ± 1.8 | 099.0 ± 0.09 | 50.0 | |
| GJ 595 AB | LHS 54 AB | 15 42 06.55 | −19 28 18.4 | new | … | *V* | 6c | 80 | 2010.16 −2015.54 | 5.39 | 11 | 106.42 ± 1.30 | 1.60 ± 0.18 | 108.02 ± 1.31 | 2256.2 ± 0.7 | 242.8 ± 0.04 | 99.0 | orbit fit |
| SCR 1546-5534 AB | | 15 46 41.84 | −55 34 47.0 | new | … | *I* | 7c | 119 | 2011.50 −2017.55 | 6.06 | 9 | 101.61 ± 0.71 | 1.50 ± 0.50 | 103.11 ± 0.87 | 421.6 ± 0.4 | 230.4 ± 0.11 | 19.4 | orbit fit, generic $\pi_{corr}$ |
| GJ 1207 | LHS 3255 | 16 57 05.73 | −04 20 56.3 | Hen06 | 6.09 | *V* | 16s | 242 | 1999.62 −2014.45 | 14.83 | 7 | 111.54 ± 0.83 | 0.75 ± 0.18 | 112.29 ± 0.85 | 607.7 ± 0.2 | 126.9 ± 0.04 | 25.7 | |
| LHS 5341 | | 18 43 06.97 | −54 36 48.4 | new | … | *R* | 10s | 119 | 2006.79 −2015.68 | 8.89 | 8 | 100.10 ± 0.99 | 1.47 ± 0.21 | 101.57 ± 1.01 | 503.7 ± 0.4 | 195.8 ± 0.08 | 23.5 | |
| SCR 1845-6357 AB | | 18 45 05.26 | −63 57 47.8 | Hen06 | 2.57 | *I* | 15c | 300 | 2003.25 −2017.72 | 14.47 | 13 | 250.63 ± 0.54 | 0.64 ± 0.05 | 251.27 ± 0.54 | 2661.4 ± 0.2 | 077.0 ± 0.01 | 50.2 | orbit fit |
| GJ 754 | LHS 60 | 19 20 47.98 | −45 33 29.7 | Jao05 | 4.06 | *V* | 15s | 194 | 1999.64 −2017.48 | 17.84 | 12 | 168.37 ± 0.94 | 2.34 ± 0.23 | 170.71 ± 0.97 | 2959.8 ± 0.2 | 168.0 ± 0.01 | 82.2 | |
| SCR 2049-4012 AB | | 20 49 09.94 | −40 12 06.2 | new | … | *R* | 8c | 148 | 2010.40 −2017.72 | 7.32 | 7 | 103.63 ± 0.87 | 0.76 ± 0.04 | 104.39 ± 0.87 | 67.9 ± 0.3 | 292.2 ± 0.54 | 3.1 | orbit fit |
| 2MA 2050-3424 | | 20 50 16.17 | −34 24 42.7 | new | … | *R* | 4c | 91 | 2012.41 −2015.82 | 3.40 | 12 | 104.18 ± 0.99 | 1.43 ± 0.16 | 105.61 ± 1.00 | 435.3 ± 0.8 | 130.2 ± 0.22 | 19.5 | |
| LHS 3746 | | 22 02 29.39 | −37 04 51.3 | Hen06 | 6.17 | *V* | 15s | 241 | 1999.71 −2017.81 | 18.11 | 10 | 131.57 ± 0.94 | 1.23 ± 0.15 | 132.80 ± 0.95 | 827.6 ± 0.2 | 105.6 ± 0.02 | 29.5 | |
| Important Additional 10 pc Members—22 Systems | | | | | | | | | | | | | | | | | | |
| GJ 54 AB | LHS 1208 AB | 01 10 22.90 | −67 26 41.9 | HIP97 | … | *V* | 18s | 259 | 2000.57 −2017.92 | 17.35 | 8 | 123.02 ± 1.99 | 1.92 ± 0.62 | 124.94 ± 2.08 | 677.0 ± 0.4 | 032.9 ± 0.06 | 25.7 | orbit fit |
| LP 991-084 | | 01 39 21.72 | −39 36 09.1 | Wei16 | … | *V* | 14s | 125 | 2003.94 −2017.92 | 13.98 | 8 | 116.61 ± 1.22 | 0.69 ± 0.09 | 117.30 ± 1.22 | 257.4 ± 0.3 | 146.5 ± 0.13 | 10.4 | Bar17 result |
| LEHPM 1-3396 | | 03 34 12.23 | −49 53 32.2 | Fah12 | … | *I* | 14s | 102 | 2004.74 −2017.93 | 13.19 | 8 | 110.63 ± 0.74 | 0.44 ± 0.13 | 111.07 ± 0.75 | 2396.8 ± 0.2 | 079.0 ± 0.01 | 102.3 | |
| LP 944-020 | | 03 39 35.25 | −35 25 43.8 | Tin96 | … | *I* | 13s | 89 | 2003.95 −2017.94 | 13.99 | 9 | 154.97 ± 0.77 | 1.36 ± 0.10 | 156.33 ± 0.78 | 406.8 ± 0.1 | 048.2 ± 0.04 | 12.3 | Die14 result |
| GJ 1103 | LHS 1951 | 07 51 54.68 | −00 00 12.6 | YPC95 | … | *V* | 14s | 149 | 2003.95 −2017.08 | 13.13 | 9 | 105.16 ± 1.00 | 0.58 ± 0.10 | 105.74 ± 1.00 | 800.4 ± 0.2 | 161.3 ± 0.02 | 35.9 | |
| GJ 299 | LHS 35 | 08 11 57.56 | +08 46 22.9 | YPC95 | … | *V* | 6s | 74 | 2010.16 −2015.06 | 4.90 | 7 | 150.06 ± 0.96 | 1.31 ± 0.18 | 151.37 ± 0.98 | 5203.2 ± 0.6 | 168.7 ± 0.01 | 162.9 | |
| 2MA 0835-0819 | | 08 35 42.53 | −08 19 23.5 | Wei16 | … | *I* | 8c | 73 | 2009.03 −2015.96 | 6.92 | 8 | 137.91 ± 0.93 | 0.42 ± 0.04 | 138.33 ± 0.93 | 607.0 ± 0.4 | 300.0 ± 0.08 | 20.8 | |
| LHS 292 | | 10 48 12.62 | −11 20 09.7 | YPC95 | … | *R* | 16s | 111 | 2000.23 −2018.15 | 17.91 | 7 | 214.05 ± 1.02 | 0.59 ± 0.04 | 214.64 ± 1.02 | 1643.6 ± 0.2 | 158.8 ± 0.01 | 36.3 | |
| GJ 406 | WOLF 359 | 10 56 28.91 | +07 00 53.2 | YPC95 | … | *R* | 14s | 162 | 2000.23 −2014.29 | 14.06 | 5 | 412.94 ± 1.46 | 1.46 ± 0.17 | 414.40 ± 1.47 | 4695.5 ± 0.4 | 236.2 ± 0.01 | 53.7 | |
| 1RXS 1159-5247 | | 11 59 27.36 | −52 47 19.0 | Sah14 | … | *I* | 8s | 78 | 2009.32 −2016.19 | 6.87 | 11 | 105.04 ± 0.69 | 1.21 ± 0.06 | 106.25 ± 0.69 | 1064.0 ± 0.4 | 262.9 ± 0.03 | 47.5 | |

**Table 1**
(Continued)

| Name (1) | Other Name (2) | R.A. J2000.0 (3) | Decl. J2000.0 (4) | Disc. Ref. (5) | Time years (6) | Filter (7) | $N_{sea}$ (8) | $N_{frm}$ (9) | Coverage (10) | Time years (11) | $N_{ref}$ (12) | $\pi$(rel) mas (13) | $\pi$(corr) mas (14) | $\pi$(abs) mas (15) | $\mu$ mas yr$^{-1}$ (16) | $\theta$ degree (17) | $V_{tan}$ km s$^{-1}$ (18) | Notes (19) |
|---|---|---|---|---|---|---|---|---|---|---|---|---|---|---|---|---|---|---|
| GJ 1154 | LHS 2351 | 12 14 16.56 | +00 37 26.4 | YPC95 | … | *V* | 6s | 50 | 2010.40 −2015.21 | 4.81 | 6 | 123.99 ± 1.83 | 0.69 ± 0.08 | 124.68 ± 1.83 | 983.7 ± 0.9 | 254.2 ± 0.09 | 37.4 | |
| SIPS 1259-4336 | | 12 59 04.77 | −43 36 24.5 | Wei16 | … | *I* | 11c | 197 | 2005.06 −2015.39 | 10.33 | 9 | 127.48 ± 0.50 | 0.45 ± 0.04 | 127.93 ± 0.50 | 1145.2 ± 0.1 | 103.7 ± 0.01 | 42.4 | |
| GJ 493.1 | LHS 2664 | 13 00 33.52 | +05 41 08.1 | YPC95 | … | *R* | 6c | 59 | 2010.16 −2015.21 | 5.05 | 5 | 113.50 ± 2.18 | 1.16 ± 0.06 | 114.66 ± 2.18 | 947.9 ± 1.2 | 283.7 ± 0.12 | 39.2 | |
| SDSS 1416 +1348 A | | 14 16 24.08 | +13 48 26.3 | Dup12 | … | *I* | 8c | 54 | 2010.40 −2017.37 | 6.97 | 10 | 105.98 ± 1.24 | 0.79 ± 0.10 | 106.77 ± 1.24 | 165.4 ± 0.6 | 036.4 ± 0.40 | 7.4 | |
| PROXIMA CEN | GJ 551 | 14 29 43.02 | −62 40 46.7 | YPC95 | … | *V* | 18s | 257 | 2000.57 −2017.55 | 16.98 | 13 | 767.99 ± 0.74 | 1.67 ± 0.37 | 769.66 ± 0.83 | 3849.2 ± 0.3 | 282.5 ± 0.01 | 23.7 | |
| LHS 3003 | | 14 56 38.26 | −28 09 48.7 | YPC95 | … | *I* | 13s | 185 | 2003.52 −2015.56 | 12.03 | 7 | 139.81 ± 0.84 | 1.63 ± 0.25 | 141.44 ± 0.88 | 969.3 ± 0.3 | 210.7 ± 0.03 | 32.5 | |
| GJ 682 | LHS 451 | 17 37 03.65 | −44 19 09.2 | YPC95 | … | *V* | 15s | 212 | 2003.52 −2017.48 | 13.96 | 8 | 201.99 ± 1.20 | 1.50 ± 0.50 | 203.49 ± 1.30 | 1165.1 ± 0.3 | 217.2 ± 0.03 | 27.1 | generic $\pi_{corr}$ |
| 2MA 1750-0016 AB | | 17 50 24.82 | −00 16 14.9 | And11 | … | *I* | 8s | 34 | 2009.55 −2017.71 | 8.16 | 19 | 110.56 ± 1.17 | 0.91 ± 0.11 | 111.47 ± 1.18 | 441.9 ± 0.4 | 296.9 ± 0.11 | 18.8 | orbit fit |
| GJ 1224 | LHS 3359 | 18 07 32.85 | −15 57 47.0 | YPC95 | … | *I* | 12s | 188 | 2003.52 −2014.66 | 11.14 | 9 | 124.95 ± 0.96 | 2.65 ± 1.56 | 127.60 ± 1.83 | 703.1 ± 0.3 | 240.9 ± 0.04 | 26.1 | |
| LP 816-060 | | 20 52 33.03 | −16 58 29.0 | HIP97 | … | *V* | 13s | 183 | 2003.52 −2016.73 | 13.21 | 8 | 174.98 ± 0.93 | 1.63 ± 0.41 | 176.61 ± 1.02 | 315.3 ± 0.2 | 277.2 ± 0.05 | 8.5 | |
| GJ 867 CD | LTT 9127 AB | 22 38 45.29 | −20 36 51.9 | YPC95 | … | *V* | 11s | 109 | 2003.52 −2014.82 | 11.30 | 5 | 109.54 ± 1.79 | 0.93 ± 0.20 | 110.47 ± 1.80 | 429.8 ± 0.5 | 096.7 ± 0.11 | 18.4 | was BD |
| LP 876-010 | | 22 48 04.50 | −24 22 07.8 | YPC95 | … | *V* | 10s | 134 | 2004.44 −2014.79 | 10.35 | 6 | 131.25 ± 1.04 | 1.02 ± 0.24 | 132.27 ± 1.07 | 378.2 ± 0.3 | 118.0 ± 0.10 | 13.6 | |
| Not 10 pc Members—9 Systems | | | | | | | | | | | | | | | | | | |
| LP 647-013 | | 01 09 51.20 | −03 43 26.4 | Cos05 | 3.20 | *I* | 12s | 93 | 2003.94 −2014.94 | 11.01 | 9 | 93.17 ± 0.85 | 0.94 ± 0.07 | 94.11 ± 0.85 | 320.9 ± 0.2 | 088.9 ± 0.06 | 16.2 | |
| LHS 1302 | | 01 51 04.09 | −06 07 05.1 | Hen06 | 6.25 | *R* | 15s | 192 | 1999.71 −2014.94 | 15.23 | 6 | 96.39 ± 0.92 | 0.64 ± 0.06 | 97.03 ± 0.92 | 597.1 ± 0.2 | 116.0 ± 0.04 | 29.2 | |
| APM 0237-5928 | | 02 36 32.46 | −59 28 05.7 | Hen06 | 6.32 | *R* | 18s | 243 | 1999.64 −2017.71 | 18.06 | 6 | 98.41 ± 0.84 | 1.34 ± 0.11 | 99.75 ± 0.85 | 723.1 ± 0.2 | 052.2 ± 0.03 | 34.4 | |
| GJ 1065 | LHS 183 | 03 50 44.29 | −06 05 41.7 | YPC95 | … | *V* | 14s | 145 | 2003.95 −2017.06 | 13.11 | 8 | 98.23 ± 1.66 | 1.31 ± 0.17 | 99.54 ± 1.67 | 1446.4 ± 0.4 | 198.9 ± 0.02 | 68.9 | |
| SCR 0717-0501 | | 07 17 17.09 | −05 01 03.6 | Fin16 | … | *I* | 12s | 134 | 2004.18 −2017.08 | 12.90 | 9 | 91.51 ± 1.61 | 1.35 ± 0.10 | 92.86 ± 1.61 | 573.8 ± 0.3 | 132.8 ± 0.06 | 29.3 | |
| 2MA 1155-3727 | | 11 55 39.53 | −37 27 35.6 | Fah12 | … | *I* | 8s | 58 | 2010.16 −2017.06 | 6.89 | 13 | 82.48 ± 1.74 | 0.28 ± 0.03 | 82.76 ± 1.74 | 789.8 ± 0.8 | 176.5 ± 0.09 | 45.2 | |
| 2MA 1645-1319 | | 16 45 22.09 | −13 19 52.2 | Fah12 | … | *I* | 9s | 84 | 2009.32 −2017.52 | 8.20 | 13 | 89.96 ± 0.79 | 0.93 ± 0.10 | 90.89 ± 0.80 | 874.2 ± 0.3 | 203.8 ± 0.04 | 45.6 | |
| 2MA 1731+2721 | | 17 31 29.75 | +27 21 23.4 | Dit14 | … | *I* | 7s | 31 | 2009.31 −2015.54 | 6.23 | 9 | 84.86 ± 1.68 | 0.68 ± 0.13 | 85.54 ± 1.69 | 265.3 ± 0.8 | 200.9 ± 0.30 | 14.7 | |
| GJ 1235 | LHS 476 | 19 21 38.70 | +20 52 03.2 | YPC95 | … | *R* | 6s | 58 | 2010.50 −2015.39 | 4.89 | 7 | 93.84 ± 1.65 | 1.50 ± 0.50 | 95.34 ± 1.72 | 1733.0 ± 0.9 | 213.7 ± 0.06 | 86.2 | generic $\pi_{corr}$ |

**References**. And11—Andrei et al. (2011), Bar17—Bartlett et al. (2017), Cos05—Costa et al. (2005), Cos06—Costa et al. (2006), Die14—Dieterich et al. (2014), Dit14—Dittmann et al. (2014), Dup12—Dupuy & Liu (2012), Fah12—Faherty et al. (2012), Fin16—Finch & Zacharias (2016), HIP97—ESA (1997), Hen06—Henry et al. (2006), Hen97—Henry et al. (1997), Jao05—Jao et al. (2005), Rie11—Riedel et al. (2011), Sah14—Sahlmann et al. (2014), Sub09—Subasavage et al. (2009), Sub17—Subasavage et al. (2017), Tin96—Tinney (1996), Wei16—Weinberger et al. (2016), YPC95—van Altena et al. (1995).

(This table is available in machine-readable form.)

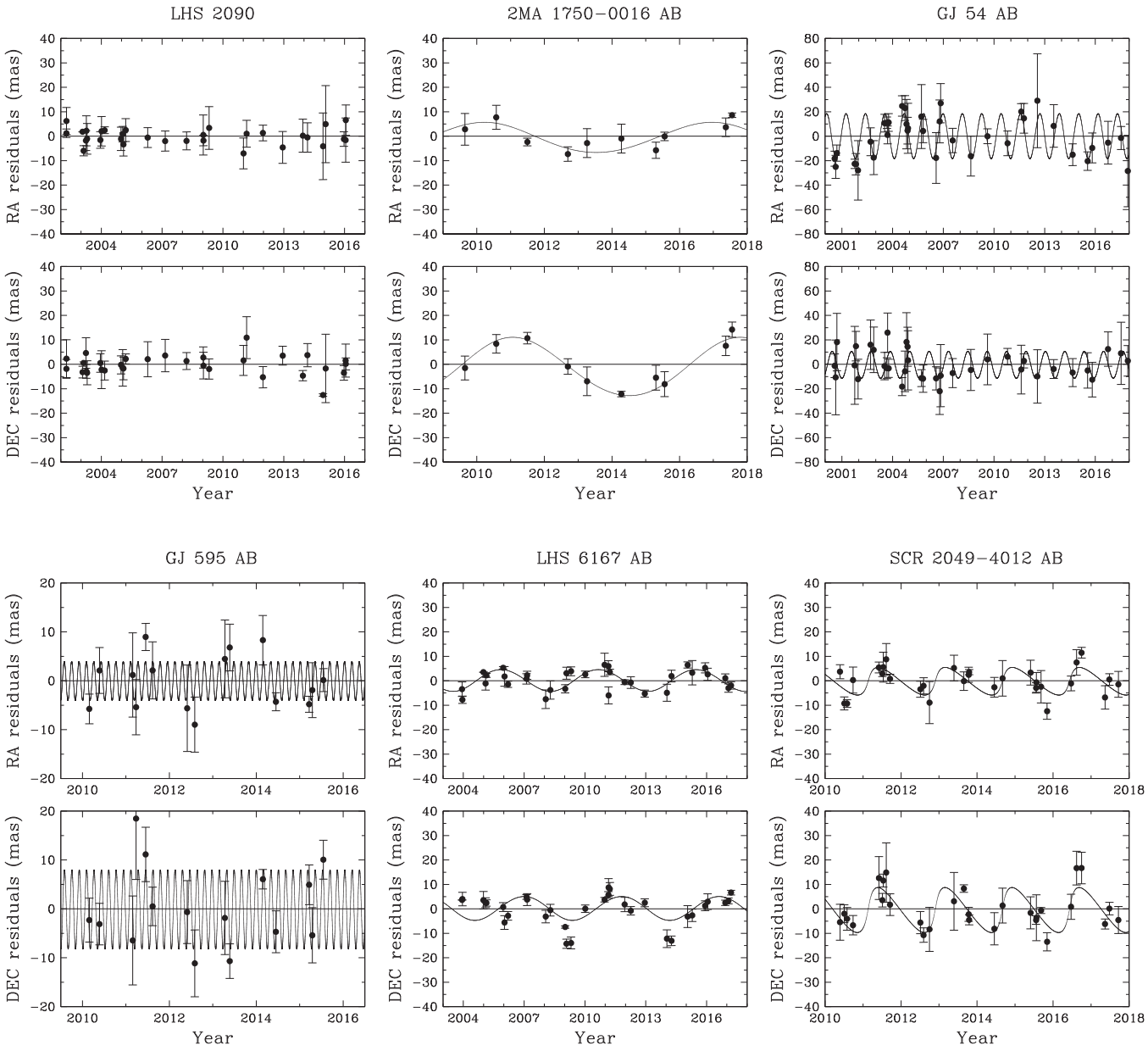


**Figure 1.** Astrometric residuals in milliarcseconds in the R.A. and decl. directions are shown for six systems, after solving for parallax and proper motion. Each point represents typically five frames taken on a single night. Note the different vertical scales that span ±20 mas to ±80 mas. The upper left panel shows flat residuals for the single star LHS 2090. The remaining panels illustrate fits to the residuals for five multiples with orbits that have wrapped in our data sets; orbital parameters are given in Table 2.

for these five systems, where for each we give the name, number of orbits covered by the current data set, orbital period ($P$), in both years and days, photocentric semimajor axis ($a$), eccentricity ($e$), inclination ($i$), longitude of periastron ($\omega$), argument of periastron ($\Omega$), and epoch of periastron ($T_0$). Errors for orbital elements are given in the second row for each system. As is often the case with astrometric data, the orbital periods are relatively well-constrained, particularly in the cases of GJ 54 AB and GJ 595 AB, for which we have data spanning many complete orbits. The photocentric semimajor axes are known to ∼10%–25% for the first four systems in Table 2. However, for each of the five orbits, the derived eccentricities, and consequently the longitudes of periastron, are poorly determined using the current data. In the worst case, the orbital period for SCR 2049-4012 AB is likely to be reliable, but because the derived inclination is nearly edge-on, we deem the rest of the elements to be suspect; additional data will be required to derive a useful orbit. Comments on these five systems with orbits are given in Section 5.

Figure 2 illustrates six more systems showing astrometric perturbations for which we do not yet have data covering complete orbits. For these systems, it is clear that close companions are present, but the orbital elements remain uncertain, so we do not provide them here. By far the largest perturbation is that of WT 460 AB, which shows shifts by more than 250 mas in both R.A. and decl. caused by a low mass stellar companion at a separation of ∼500 mas. Comments on each of these six systems are also given in Section 5.

**Table 2**
Photocentric Orbits for Nearby Systems

| Name | #orbits | $P$ (year) | $P$ (day) | $a$ (mas) | $e$ | $i$ (degree) | $\omega$ (degree) | $\Omega$ (degree) | $T_0$ |
|---|---|---|---|---|---|---|---|---|---|
| (1) | (2) | (3) | (4) | (5) | (6) | (7) | (8) | (9) | |
| 2MA 1750-0016 AB | 1.2 | 6.74 | 2460.4 | 12.7 | 0.08 | 110.0 | 339.0 | 21.5 | 2024.04 |
| | | 0.39 | 143.5 | 1.2 | 0.09 | 7.3 | 83.4 | 8.3 | 1.60 |
| GJ 54 AB | 15.1 | 1.15 | 419.1 | 18.7 | 0.04 | 124.2 | 102.0 | 102.3 | 2018.75 |
| | | <0.01 | 1.3 | 1.9 | 0.05 | 7.7 | 73.7 | 9.7 | 0.24 |
| GJ 595 AB | 31.8 | 0.17 | 62.0 | 9.0 | 0.02 | 94.5 | 217.9 | 205.9 | 2018.43 |
| | | <0.01 | 0.1 | 2.2 | 0.14 | 5.8 | 112.5 | 13.2 | 0.22 |
| LHS 6167 AB | 2.8 | 4.81 | 1755.9 | 5.0 | 0.04 | 149.3 | 352.0 | 206.2 | 2018.59 |
| | | 0.13 | 46.6 | 0.7 | 0.09 | 25.1 | 104.9 | 46.9 | 1.33 |
| SCR 2049-4012 AB | 4.1 | 1.77 | 644.9 | 13.7 | 0.61 | 89.5 | 93.3 | 211.6 | 2018.20 |
| | | 0.02 | 7.1 | 7.8 | 0.94 | 1.0 | 1.4 | 6.8 | 0.06 |

### 4.2. Photometry

Photometry results in the *VRIJHK* filters are given in Table 3, where variability measurements are also listed. Some of our *VRI* photometry has been published in previous papers in this series (e.g., Winters et al. 2015), but here we list RECONS values with the number of nights of data rather than the individual references, including updated values when additional nights of *VRI* data have been acquired. Thus, values given here supersede previously published values for these objects.

Table 3 lists names for the systems (column 1), coordinates (2, 3), *VRI* photometry (4, 5, 6), and the number of observations (7), where the three digits indicate the numbers of nights in which magnitudes were measured in the *VRI* bands, respectively. Note that fainter objects sometimes have limited $V$ measurements. The next columns give the filter in which the images used for both astrometry and variability were taken (8) and the variability in millimagnitudes in that filter (9). These results are followed by the 2MASS *JHK* magnitudes (10, 11, 12), the spectral types, luminosity classes, and references (13, 14, 15) and notes (16). The indicator "J" beside *VRIJHK* photometric values and spectral types is used to represent joint measurements of two or more components.

The level of variability in millimagnitudes (mmag) in the parallax filter listed in column (9) of Table 2 has been derived as described in previous papers in this series—in particular, Jao et al. (2011), Hosey et al. (2015), and Clements et al. (2017). The method outlined in Honeycutt (1992) has been used to derive the nightly offsets and zero points for relative instrumental photometry to derive stellar variability.

Among the 75 components with variability measurements, 11 vary by more than 20 mmag (2%), our adopted cutoff for a clearly variable star, as described in Hosey et al. (2015). We interpret variability above 20 mmag to be due to spots that move in and out of view as a star rotates on short timescales and/or that come and go over decades in the form of stellar spot cycles. Note that even below 20 mmag, some stars show evidence of clear brightness changes, at least down to 15 mmag in our data. Light curves for 12 of the most compelling cases are shown in Figure 3 and Figure 4, and can be broken into three subsets:

*Cycles:* Remarkable among the observed stars are several that show clear evidence of long-term stellar cycles. Light curves for six stars are shown in Figure 3, with cycles that last 7–15 years. The clearest example is GJ 1128 (20.5 mmag in $V$), with a 5-year cycle for which we see more than two cycles.

*Trends:* The top four panels of Figure 4 show light curves for stars exhibiting long-term trends that may be portions of cycles extending beyond the current data sets. In particular, the closest pre-main sequence star (Riedel et al. 2011) AP Col (22.9 mmag in $V$) shows evidence of a brightening trend of nearly 10% from 2007 to 2018 due to a long-term cycle, upon which are superimposed significant short-term variations presumably due to spots. WT 460 AB (18.8 mag in $I$) also shows a clear trend, having grown fainter by 6% from 2000 to 2013 and brightening since.

*Spots:* The bottom two panels of Figure 4 show light curves for the two most extreme cases of variability in the sample—the close binary GJ 867 CD (31.5 mmag at $V$), which has an orbital period of 1.8 days (see Section 5), and Proxima Centauri (36.5 mmag at $V$). In fact, with the largest variability measurement in the sample, Proxima Centauri shows substantial changes in brightness throughout the 17 years of observations.

### 4.3. Spectroscopy

Spectral types and luminosity classes are given in Table 3, along with references. Nearly all of the systems in this paper have primaries that are M dwarfs for which we provide updated types, indicated with asterisks in column (15) of Table 3. As described in Section 3.3, the M types presented here supersede types given in previous papers in this series. For the few stars that we did not observe, types are taken from the literature, or for those that have no spectroscopic observations, we estimate the type based on the star's $V - K$ color and give "estim" as the reference. As with the photometry, a "J" is listed (in the luminosity class column) when the light of two or more close components was merged in the spectrum used for typing.

Among the 44 systems added by RECONS, there are 31 with types M3V–M5V, as is typical for the solar neighborhood population. There are a few objects that are not main-sequence M dwarfs. The pre-main sequence star, AP Col, is noted as

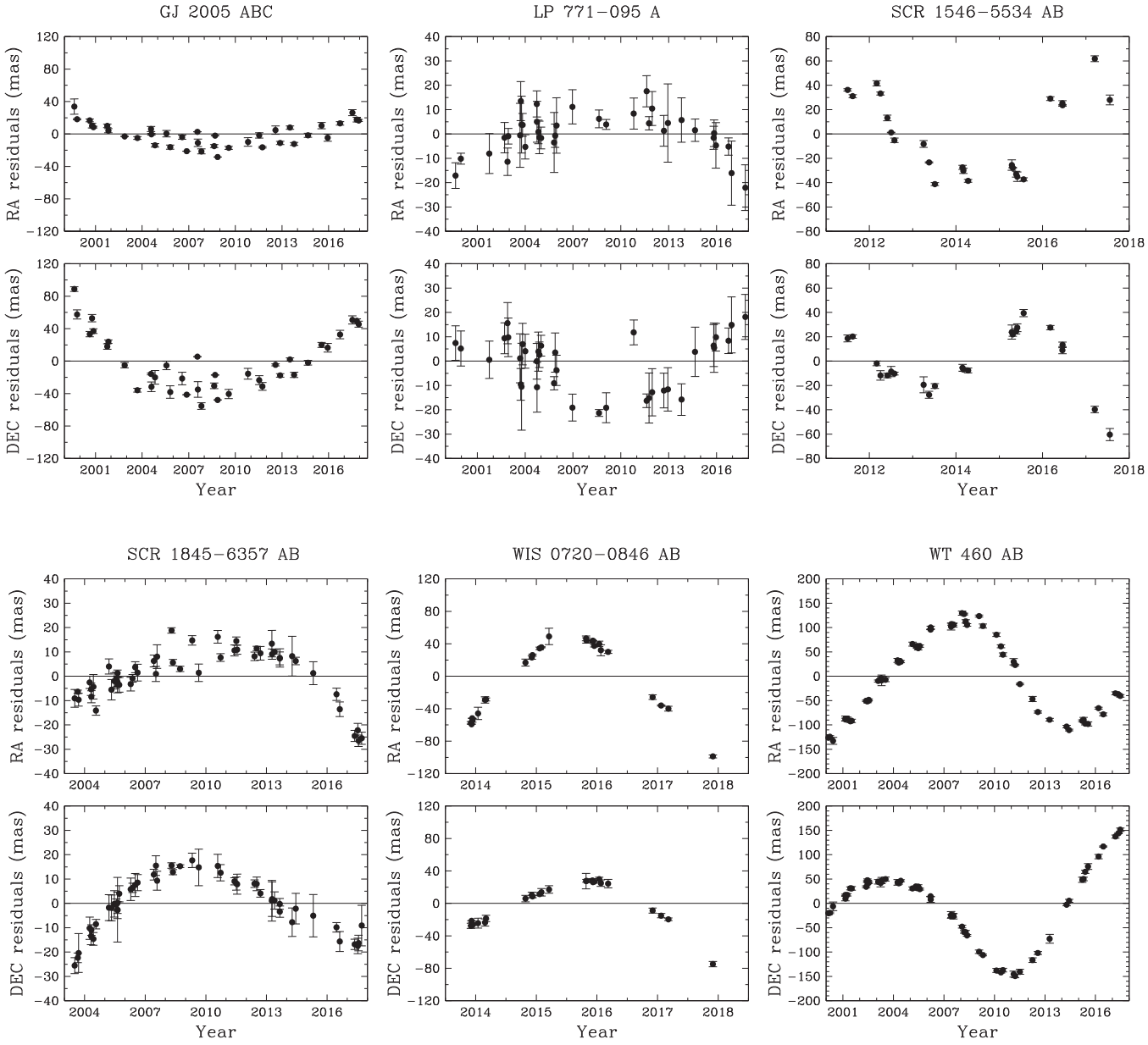


**Figure 2.** Astrometric residuals in milliarcseconds in the R.A. and decl. directions are shown for six systems, after solving for parallax and proper motion. Each point represents typically five frames taken on a single night. Note the different vertical scales that span ±40 mas to ±200 mas. All six systems show clear evidence of photocentric perturbations, but none have yet wrapped into closed orbits in our data sets.

luminosity class "pms" rather than "V." Types for the two white dwarfs are DQpec for WD 0038-226 from Giammichele et al. (2012), and DAZ for WD 0141-675 from Debes & Kilic (2010); further details about the white dwarf spectral types can be found in Subasavage et al. (2017).

## 5. Systems Worthy of Note

Here we provide additional details for many of the systems presented in this paper, including the 14 new 10 pc systems and each of the 17 multiple systems. For ease of use, all notes on systems are collected in this section and are ordered by R.A. (position given in italics). In the descriptions below, our photometric distance estimates are from two sources. We use SuperCOSMOS *BRI* magnitudes derived from photographic plate scans combined with 2MASS *JHK* to estimate distances accurate to 26%, as described in Hambly et al. (2004). Similarly, we use our own *VRI* photometry, primarily from the 0.9 m, combined with 2MASS *JHK* to estimate distances accurate to 15%, as described in Henry et al. (2004). In particular, offsets between these photometrically estimated distances and the trigonometric distances often reveal flux contributed by unseen companions.

1. *0024−2708*: *GJ 2005 ABC* first entered the 10 pc sample in Costa et al. (2005) with $\pi_{\rm trig} = 129.47 \pm 2.48$ mas based on 2.3 years of 1.5 m data, targeted primarily because the YPC value of $\pi_{\rm trig} = 135.3 \pm 12.1$ mas had an error larger than 10 mas. From the 0.9 m we present a new value of $\pi_{\rm trig} = 139.30 \pm 1.59$ mas using 18.3 years of data after taking into account the notable curvature due to orbital motion of BC around A shown in Figure 2. As a check of the new larger parallax, a reduction using only data from 2013 to 2016 was done to minimize the effect

**Table 3**
Photometric and Spectroscopic Results

| Name | R.A. J2000.0 | Decl. J2000.0 | $V$ | | $R$ | | $I$ | | # | $\pi$ | $\sigma$ | $J$ | | $H$ | | $K$ | | Spec | Lum | Spec | Notes |
|---|---|---|---|---|---|---|---|---|---|---|---|---|---|---|---|---|---|---|---|---|---|
| | | | mag | | mag | | mag | | nts | filter | mmag | mag | | mag | | mag | | Type | Class | Ref | |
| (1) | (2) | (3) | (4) | | (5) | | (6) | | (7) | (8) | (9) | (10) | | (11) | | (12) | | (13) | (14) | (15) | (16) |
| New 10 pc Members—44 Systems | | | | | | | | | | | | | | | | | | | | | |
| GJ 2005 ABC | 00 24 44.19 | −27 08 24.2 | 15.28 | J | 13.52 | J | 11.37 | J | 665 | *R* | 17.2 | 9.25 | J | 8.55 | J | 8.24 | J | M5.5 | VJ | * | ABC <2″ |
| WD 0038-226 | 00 41 26.03 | −22 21 02.3 | 14.50 | | 14.08 | | 13.67 | | 444 | *R* | 7.4 | 13.34 | | 13.48 | | 13.74 | | DQ | pec | Sub17 | |
| WD 0141-675 | 01 43 00.98 | −67 18 30.4 | 13.82 | | 13.52 | | 13.23 | | 333 | *V* | 6.4 | 12.87 | | 12.66 | | 12.58 | | DAZ | | Sub17 | |
| L 173-019 | 02 00 38.31 | −55 58 04.8 | 11.90 | | 10.70 | | 9.15 | | 333 | *V* | 19.9 | 7.63 | | 7.09 | | 6.77 | | M2.0 | V | * | |
| SO 0253+1652 | 02 53 00.89 | +16 52 52.7 | 15.14 | | 13.03 | | 10.65 | | 333 | *I* | 10.3 | 8.39 | | 7.88 | | 7.59 | | M6.5 | V | * | |
| DEN 0255-4700 | 02 55 03.68 | −47 00 51.6 | 22.92 | | 19.91 | | 17.45 | | 111 | *I* | … | 13.25 | | 12.20 | | 11.56 | | L8 | | Fil15 | from Cos06 |
| LTT 1445 A | 03 01 51.04 | −16 35 31.0 | 11.22 | | 10.07 | | 8.66 | | 444 | *V* | 17.6 | 7.29 | | 6.77 | | 6.50 | | M2.5 | V | * | A-BC 7″ |
| LTT 1445 BC | 03 01 51.04 | −16 35 31.0 | 11.37 | J | 10.13 | J | 8.58 | J | 444 | *V* | 15.9 | 7.11 | J | 6.56 | J | 6.29 | J | M3.0 | VJ | * | BC 1.″3 |
| GJ 1061 | 03 35 59.72 | −44 30 45.5 | 13.09 | | 11.45 | | 9.47 | | 666 | *R* | 20.0 | 7.52 | | 7.02 | | 6.61 | | M5.0 | V | * | |
| LHS 1610 AB | 03 52 41.76 | +17 01 04.3 | 13.85 | J | 12.42 | J | 10.66 | J | 555 | *V* | 29.1 | 8.93 | J | 8.38 | J | 8.05 | J | M4.0 | VJ | * | AB <1″ |
| GJ 1068 | 04 10 28.14 | −53 36 08.2 | 13.60 | | 12.18 | | 10.42 | | 333 | *R* | 14.0 | 8.75 | | 8.21 | | 7.90 | | M4.0 | V | * | |
| LHS 1723 | 05 01 57.43 | −06 56 46.5 | 12.20 | | 10.86 | | 9.18 | | 444 | *V* | 19.5 | 7.62 | | 7.07 | | 6.74 | | M4.0 | V | * | |
| LTT 17736 | 05 04 14.76 | +11 03 23.8 | 13.76 | | 12.43 | | 10.74 | | 443 | *R* | 11.1 | 9.14 | | 8.61 | | 8.31 | | M4.5 | V | * | |
| GJ 203 | 05 28 00.15 | +09 38 38.2 | 12.46 | | 11.27 | | 9.78 | | 333 | *V* | 15.1 | 8.31 | | 7.84 | | 7.54 | | M3.0 | V | * | |
| LTT 17897 | 06 00 03.52 | +02 42 23.6 | 11.31 | | 10.04 | | 8.43 | | 665 | *V* | 16.6 | 6.91 | | 6.31 | | 6.04 | | M3.5 | V | * | |
| AP COL | 06 04 52.16 | −34 33 36.0 | 12.98 | | 11.50 | | 9.60 | | 777 | *V* | 22.9 | 7.74 | | 7.18 | | 6.87 | | M4.5 | pms | * | pre-main sequence star |
| SCR 0630-7643 AB | 06 30 46.61 | −76 43 08.9 | 14.82 | J | 13.08 | J | 11.00 | J | 444 | *I* | 6.7 | 8.89 | J | 8.28 | J | 7.92 | J | M5.0 | VJ | * | AB <1″ |
| WIS 0720-0846 AB | 07 20 03.25 | −08 46 50.0 | 18.54 | J | 16.24 | J | 13.89 | J | 444 | *I* | 14.3 | 10.63 | J | 9.92 | J | 9.47 | J | M9.5 | VJ | Bur15 | AB <1″ |
| LTT 17993 AB | 07 36 25.13 | +07 04 43.1 | 13.25 | J | 11.81 | J | 9.97 | J | 444 | *R* | 14.0 | 8.18 | J | 7.61 | J | 7.28 | J | M4.5 | VJ | * | AB <1″ |
| SCR 0740-4257 | 07 40 11.80 | −42 57 40.3 | 13.81 | | 12.36 | | 10.50 | | 333 | *R* | 15.0 | 8.68 | | 8.09 | | 7.77 | | M4.5 | V | * | |
| GJ 300 | 08 12 40.88 | −21 33 06.8 | 12.14 | | 10.85 | | 9.22 | | 444 | *V* | 16.6 | 7.60 | | 6.96 | | 6.71 | | M3.5 | V | * | |
| UPM 0815-2344 AB | 08 15 11.19 | −23 44 15.7 | 12.36 | J | 11.16 | J | 9.62 | J | 333 | *V* | 12.0 | 8.11 | J | 7.51 | J | 7.22 | J | M3.5 | VJ | estim | AB <2″ |
| L 098-059 | 08 18 07.63 | −68 18 46.9 | 11.71 | | 10.61 | | 9.25 | | 333 | *R* | 11.2 | 7.93 | | 7.36 | | 7.10 | | M2.5 | V | * | |
| LTT 12352 ABC | 08 58 56.33 | +08 28 26.0 | 10.92 | J | 9.67 | J | 8.05 | J | 333 | *V* | 15.4 | 6.51 | J | 5.97 | J | 5.69 | J | M3.5 | VJ | * | ABC <1″ |
| LHS 2090 | 09 00 23.55 | +21 50 04.8 | 16.11 | | 14.12 | | 11.84 | | 333 | *I* | 11.5 | 9.44 | | 8.84 | | 8.44 | | M6.0 | V | * | |
| LHS 6167 AB | 09 15 36.40 | −10 35 47.2 | 13.82 | J | 12.32 | J | 10.42 | J | 333 | *V* | 28.5 | 8.61 | J | 8.07 | J | 7.73 | J | M4.5 | VJ | * | AB <1″ |
| GJ 1123 | 09 17 05.33 | −77 49 23.4 | 13.15 | | 11.79 | | 10.05 | | 333 | *V* | 27.4 | 8.33 | | 7.77 | | 7.45 | | M4.0 | V | * | |
| GJ 1128 | 09 42 46.36 | −68 53 06.1 | 12.74 | | 11.36 | | 9.62 | | 333 | *V* | 20.5 | 7.95 | | 7.39 | | 7.04 | | M4.0 | V | * | |
| LHS 2206 | 09 53 55.19 | +20 56 46.8 | 14.02 | | 12.63 | | 10.85 | | 333 | *R* | 17.1 | 9.21 | | 8.60 | | 8.33 | | M4.0 | V | * | |
| LHS 288 | 10 44 21.24 | −61 12 35.6 | 13.90 | | 12.31 | | 10.27 | | 333 | *R* | 11.5 | 8.49 | | 8.05 | | 7.73 | | M5.0 | V | * | |
| DENIS 1048-3956 | 10 48 14.56 | −39 56 07.0 | 17.39 | | 14.99 | | 12.48 | | 555 | *I* | 10.7 | 9.54 | | 8.91 | | 8.45 | | M8.5 | V | * | |
| SCR 1138-7721 | 11 38 16.76 | −77 21 48.5 | 14.78 | | 13.20 | | 11.24 | | 444 | *I* | 8.3 | 9.40 | | 8.89 | | 8.52 | | M5.0 | V | * | |
| SIPS 1141-3624 | 11 41 21.52 | −36 24 34.7 | 13.10 | | 11.79 | | 10.10 | | 333 | *R* | 16.2 | 8.49 | | 7.97 | | 7.70 | | M4.0 | V | * | |
| LHS 337 | 12 38 49.10 | −38 22 53.8 | 12.75 | | 11.44 | | 9.74 | | 333 | *R* | 9.9 | 8.17 | | 7.76 | | 7.39 | | M4.0 | V | * | |
| WT 460 AB | 14 11 59.93 | −41 32 21.3 | 15.68 | J | 13.93 | J | 11.81 | J | 666 | *I* | 18.8 | 9.67 | J | 9.04 | J | 8.62 | J | M5.0 | VJ | * | AB <1″ |
| WIS 1540-5101 | 15 40 43.52 | −51 01 35.9 | 15.34 | | 13.40 | | 11.19 | | 333 | *R* | 12.4 | 8.96 | | 8.30 | | 7.94 | | M7.0 | V | Per14 | |
| GJ 595 AB | 15 42 06.55 | −19 28 18.4 | 11.84 | J | 10.73 | J | 9.29 | J | 333 | *V* | 9.5 | 7.92 | J | 7.42 | J | 7.17 | J | M3.0 | VJ | * | AB <1″ |
| SCR 1546-5534 AB | 15 46 41.84 | −55 34 47.0 | 17.63 | J | 15.40 | J | 12.99 | J | 555 | *I* | 11.5 | 10.21 | J | 9.55 | J | 9.11 | J | M7.5 | VJ | Raj13 | AB <1″ |
| GJ 1207 | 16 57 05.73 | −04 20 56.3 | 12.25 | | 10.99 | | 9.43 | | 555 | *V* | 18.1 | 7.97 | | 7.44 | | 7.12 | | M3.5 | V | * | |
| LHS 5341 | 18 43 06.97 | −54 36 48.4 | 12.97 | | 11.68 | | 10.03 | | 333 | *R* | 16.5 | 8.42 | | 7.79 | | 7.49 | | M4.0 | V | * | |
| SCR 1845-6357 AB | 18 45 05.26 | −63 57 47.8 | 17.40 | J | 14.99 | J | 12.46 | J | 555 | *I* | 9.7 | 9.54 | J | 8.97 | J | 8.51 | J | M8.5 | VJ | * | AB <1″ |
| GJ 754 | 19 20 47.98 | −45 33 29.7 | 12.25 | | 10.94 | | 9.25 | | 333 | *V* | 13.5 | 7.66 | | 7.13 | | 6.85 | | M4.0 | V | * | |

**Table 3**
(Continued)

| Name | R.A. | Decl. | $V$ | | $R$ | | $I$ | | # | $\pi$ | $\sigma$ | $J$ | | $H$ | | $K$ | | Spec | Lum | Spec | Notes |
|---|---|---|---|---|---|---|---|---|---|---|---|---|---|---|---|---|---|---|---|---|---|
| | J2000.0 | J2000.0 | mag | | mag | | mag | | nts | filter | mmag | mag | | mag | | mag | | Type | Class | Ref | |
| (1) | (2) | (3) | (4) | | (5) | | (6) | | (7) | (8) | (9) | (10) | | (11) | | (12) | | (13) | (14) | (15) | (16) |
| SCR 2049-4012 AB | 20 49 09.94 | −40 12 06.2 | 13.53 | J | 12.12 | J | 10.31 | J | 333 | *R* | 17.8 | 8.60 | J | 8.02 | J | 7.70 | J | M4.5 | VJ | * | AB <1″ |
| 2MA 2050-3424 | 20 50 16.17 | −34 24 42.7 | 13.75 | | 12.31 | | 10.55 | | 333 | *R* | 8.1 | 8.82 | | 8.27 | | 8.00 | | M4.0 | V | estim | |
| LHS 3746 | 22 02 29.39 | −37 04 51.3 | 11.76 | | 10.56 | | 9.04 | | 444 | *V* | 13.2 | 7.60 | | 7.02 | | 6.72 | | M3.0 | V | * | |
| Important Additional 10 pc Members—22 Systems | | | | | | | | | | | | | | | | | | | | | |
| GJ 54 AB | 01 10 22.90 | −67 26 41.9 | 9.82 | J | 8.70 | J | 7.32 | J | 555 | *V* | 15.8 | 6.00 | J | 5.41 | J | 5.13 | J | M2.5 | VJ | * | AB <1″ |
| LP 991-084 | 01 39 21.72 | −39 36 09.1 | 14.48 | | 12.97 | | 11.06 | | 333 | *V* | 14.2 | 9.21 | | 8.63 | | 8.27 | | M4.5 | V | * | |
| LEHPM 1-3396 | 03 34 12.23 | −49 53 32.2 | 19.38 | | 16.85 | | 14.39 | | 333 | *I* | 9.6 | 11.38 | | 10.82 | | 10.39 | | M9.0 | V | * | |
| LP 944-020 | 03 39 35.25 | −35 25 43.8 | 18.70 | | 16.39 | | 14.00 | | 333 | *I* | 8.6 | 10.73 | | 10.02 | | 9.55 | | M9.0 | V | * | |
| GJ 1103 | 07 51 54.68 | −00 00 12.6 | 13.26 | | 11.89 | | 10.19 | | 333 | *V* | 15.8 | 8.50 | | 7.94 | | 7.66 | | M4.5 | V | * | |
| GJ 299 | 08 11 57.56 | +08 46 22.9 | 12.86 | | 11.57 | | 9.91 | | 333 | *V* | 13.3 | 8.42 | | 7.93 | | 7.66 | | M3.5 | V | * | |
| 2MA 0835-0819 | 08 35 42.53 | −08 19 23.5 | 22.97 | | 19.33 | | 17.00 | | 144 | *I* | 23.2 | 13.17 | | 11.94 | | 11.14 | | L5 | | Fil15 | |
| LHS 292 | 10 48 12.62 | −11 20 09.7 | 15.78 | | 13.63 | | 11.25 | | 333 | *R* | 12.5 | 8.86 | | 8.26 | | 7.93 | | M6.5 | V | * | |
| GJ 406 | 10 56 28.91 | +07 00 53.2 | 13.61 | | 11.66 | | 9.46 | | 333 | *R* | 16.3 | 7.09 | | 6.48 | | 6.08 | | M5.5 | V | * | |
| 1RXS 1159-5247 | 11 59 27.36 | −52 47 19.0 | 19.14 | | 16.92 | | 14.49 | | 333 | *I* | 12.0 | 11.43 | | 10.76 | | 10.32 | | M9.0 | V | Ham04 | |
| GJ 1154 | 12 14 16.56 | +00 37 26.4 | 13.66 | | 12.17 | | 10.31 | | 333 | *V* | 14.9 | 8.46 | | 7.86 | | 7.54 | | M4.5 | V | * | |
| SIPS 1259-4336 | 12 59 04.77 | −43 36 24.5 | 18.01 | | 15.74 | | 13.29 | | 333 | *I* | 12.2 | 10.53 | | 9.95 | | 9.52 | | M7.5 | V | estim | |
| GJ 493.1 | 13 00 33.52 | +05 41 08.1 | 13.43 | | 12.04 | | 10.27 | | 333 | *R* | 15.7 | 8.55 | | 7.97 | | 7.66 | | M4.5 | V | * | |
| SDSS 1416+1348 A | 14 16 24.08 | +13 48 26.3 | … | | 19.37 | | 16.84 | | 044 | *I* | 18.8 | 13.15 | | 12.46 | | 12.11 | | L5 | | Sch10 | values for A only |
| PROXIMA CEN | 14 29 43.02 | −62 40 46.7 | 11.13 | | 9.45 | | 7.41 | | 333 | *V* | 36.5 | 5.36 | | 4.84 | | 4.38 | | M5.0 | V | * | |
| LHS 3003 | 14 56 38.26 | −28 09 48.7 | 16.98 | | 14.91 | | 12.55 | | 444 | *I* | 11.9 | 9.97 | | 9.32 | | 8.93 | | M6.5 | V | * | |
| GJ 682 | 17 37 03.65 | −44 19 09.2 | 10.99 | | 9.74 | | 8.15 | | 333 | *V* | 12.1 | 6.54 | | 5.92 | | 5.61 | | M4.0 | V | * | |
| 2MA 1750-0016 AB | 17 50 24.82 | −00 16 14.9 | 21.32 | J | 19.15 | J | 16.92 | J | 133 | *I* | 29.3 | 13.29 | J | 12.41 | J | 11.85 | J | L5 | J | Ken07 | AB <1″ |
| GJ 1224 | 18 07 32.85 | −15 57 47.0 | 13.51 | | 12.11 | | 10.32 | | 333 | *I* | 11.5 | 8.64 | | 8.09 | | 7.83 | | M4.0 | V | * | |
| LP 816-060 | 20 52 33.03 | −16 58 29.0 | 11.50 | | 10.25 | | 8.64 | | 333 | *V* | 18.7 | 7.09 | | 6.52 | | 6.20 | | M3.0 | V | * | |
| GJ 867 CD | 22 38 45.29 | −20 36 51.9 | 11.47 | J | 10.29 | J | 8.77 | J | 333 | *V* | 31.5 | 7.34 | J | 6.82 | J | 6.49 | J | M3.5 | VJ | * | CD <1″ |
| LP 876-010 | 22 48 04.50 | −24 22 07.8 | 12.62 | | 11.32 | | 9.63 | | 444 | *V* | 13.1 | 8.08 | | 7.53 | | 7.21 | | M4.0 | V | * | |
| Not 10 pc Members—9 Systems | | | | | | | | | | | | | | | | | | | | | |
| LP 647-013 | 01 09 51.20 | −03 43 26.4 | 19.35 | | 17.13 | | 14.87 | | 444 | *I* | 8.9 | 11.69 | | 10.93 | | 10.43 | | M9.0 | V | * | |
| LHS 1302 | 01 51 04.09 | −06 07 05.1 | 14.49 | | 13.00 | | 11.16 | | 555 | *R* | 20.2 | 9.41 | | 8.84 | | 8.55 | | M4.5 | V | * | |
| APM 0237-5928 | 02 36 32.46 | −59 28 05.7 | 14.47 | | 12.96 | | 11.08 | | 555 | *R* | 15.6 | 9.28 | | 8.70 | | 8.34 | | M5.0 | V | * | |
| GJ 1065 | 03 50 44.29 | −06 05 41.7 | 12.82 | | 11.60 | | 10.04 | | 333 | *V* | 19.1 | 8.57 | | 8.00 | | 7.75 | | M3.5 | V | * | |
| SCR 0717-0501 | 07 17 17.09 | −05 01 03.6 | 13.30 | | 12.02 | | 10.40 | | 444 | *I* | 11.0 | 8.87 | | 8.35 | | 8.05 | | M4.0 | V | * | |
| 2MA 1155-3727 | 11 55 39.53 | −37 27 35.6 | 20.95 | | 18.38 | | 16.17 | | 344 | *I* | 17.2 | 12.81 | | 12.04 | | 11.46 | | L2 | V | Fil15 | |
| 2MA 1645-1319 | 16 45 22.09 | −13 19 52.2 | 20.60 | | 17.97 | | 15.72 | | 555 | *I* | 12.2 | 12.45 | | 11.69 | | 11.15 | | L1.5 | V | Giz02 | |
| 2MA 1731+2721 | 17 31 29.75 | +27 21 23.4 | 19.86 | | 17.67 | | 15.36 | | 133 | *I* | 9.6 | 12.09 | | 11.39 | | 10.91 | | L0 | V | Rei08 | |
| GJ 1235 | 19 21 38.70 | +20 52 03.2 | 13.48 | | 12.14 | | 10.47 | | 333 | *R* | 14.2 | 8.80 | | 8.22 | | 7.94 | | M4.0 | V | * | |

**Note**. A "J" next to a magnitude or spectral type indicates that more than one object is included in the measurement value (i.e., a close multiple system).

**References**. *—this paper, Bur15—Burgasser et al. (2015), Cos06—Costa et al. (2006), Fil15—Filippazzo et al. (2015), Giz02—Gizis (2002), Ham04—Hambaryan et al. (2004), Ken07—Kendall et al. (2007), Per14—Pérez Garrido et al. (2014), Raj13—Rajpurohit et al. (2013), Rei08—Reid et al. (2008), Sch10—Schmidt et al. (2010), Sub17—Subasavage et al. (2017) .

(This table is available in machine-readable form.)

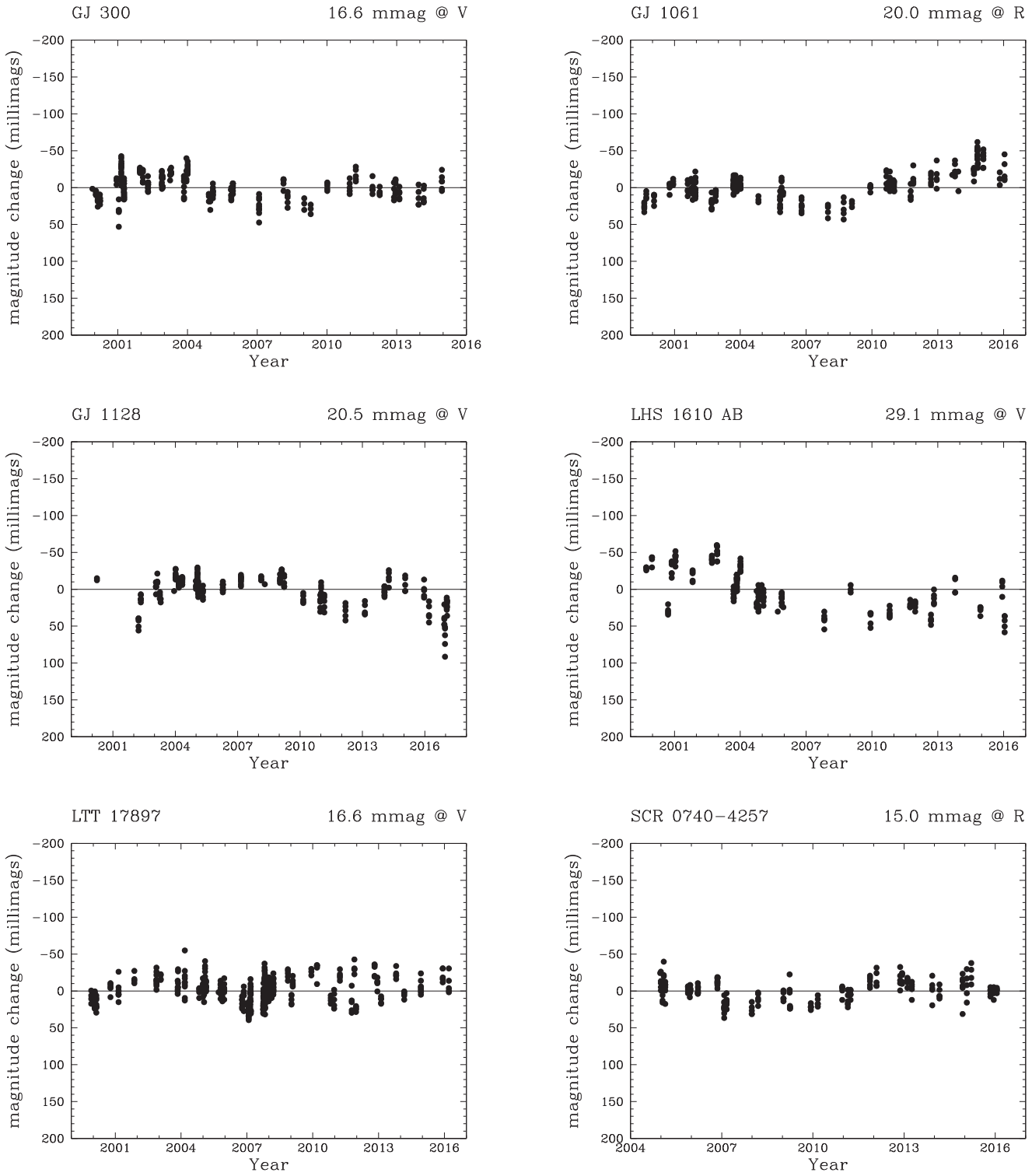


**Figure 3.** Photometric variability levels are shown for six stars with cycles lasting 7–15 years observed at the 0.9 m. Points represent brightnesses in single frames and are shown oriented so that a star moves up on the plot when it grows brighter. Star names, variability measurements, and the filters used for the observations are given at the top of each panel. Complete cycles are evident for all stars except LHS 1610 AB, which may have been overluminous from 2000 to 2004, followed by a complete cycle from 2004 to 2014.

of the orbital curvature, and a consistent parallax was found. The orbital fit is only a guide, given that the orbital period of BC around A is likely a century or more, while the BC pair has an orbital period of 16.1 years (Leinert et al. 2001). With masses of 0.07–0.08 $M_{\odot}$ (see Benedict et al. 2016), the B and C components are crucial to our understanding of the transition region between stars and brown dwarfs. The combined light from the three components exhibits a variation in the *R* band with a period ∼13 years.

2. *0109−0343*: *LP 647-013* was reported in Costa et al. (2005) to have $\pi_{\rm trig} = 104.23 \pm 2.29$ mas from our program at the

CTIO 1.5 m, using data spanning 3.2 years. Weinberger et al. (2016) recently measured $\pi_{\rm trig} = 97.55 \pm 2.04$ mas, and when combined with our new value from the 0.9 m program, $\pi_{\rm trig} = 94.11 \pm 0.85$ mas using data spanning 11.0 years, this M9.0V star is pushed beyond 10 pc.

3. *0110−6726*: *GJ 54 AB* was suspected to be a binary by Rodgers & Eggen (1974) and was confirmed to be a close pair of red dwarfs by Golimowski et al. (2004), who imaged the secondary using *HST*'s Fine Guidance Sensors (FGS) and *HST*'s Near Infrared Camera and Multi-Object Spectrometer (NICMOS). Continuing work by RECONS using *HST*-FGS indicates a parallax of $126.9 \pm 0.4$ mas, an orbital period of 418.5 days (1.15 years), semimajor axis of the relative (not photocentric) orbit of 126.4 mas, $\Delta V = 1.04$ mag, and masses of 0.43 and 0.30 $M_{\odot}$ (Benedict et al. 2016). The system provides a classic case of orbit entanglement that wreaks havoc on parallax measurements because the orbital period nearly matches the 1.00 year period of parallactic motion. Although observed using faint reference stars and only averaging 20 s per integration, after more than 15 orbital cycles covered in our astrometry program over 17.4 years, we fit for the orbital motion (see Table 2 and Figure 1), finding $P_{\rm orb} = 419.1 \pm 1.3$ days, consistent with the FGS orbit. The resulting $\pi_{\rm trig} = 124.94 \pm 2.08$ mas is more reliable than the early value in Henry et al. (2006), which was undoubtedly corrupted by the orbital motion. The matching parallaxes from the 0.9 m and *HST* indicate a semimajor axis for the orbiting pair of almost precisely 1.00 au.
4. *0151−0607*: *LHS 1302* was reported in Henry et al. (2006) to have $\pi_{\rm trig} = 100.78 \pm 1.89$ mas, placing it near the 10 pc border. Additional data extend the coverage from 6.2 years to 15.2 years, resulting in a new value of $\pi_{\rm trig} = 97.03 \pm 0.92$ mas (10.3 pc). The star was reported in Riedel et al. (2014) to be a potential kinematic match to the ∼30 Myr old Columba association, although its surface gravity and isochrone placement suggest it is a field object. It is not noticeably elevated from the main sequence, but was observed to flare by 0.15 mag in the *R* band on UT 2004 November 22.
5. *0200−5558*: *L 173-019* is a new low-proper-motion ($\mu = 126$ mas yr$^{-1}$) member of the solar neighborhood at only 8.1 pc. This is one of four new systems reported here with proper motions less than 200 mas yr$^{-1}$, ranking fourth slowest within 10 pc. The reference stars are faint compared to L 173-019 ($V = 11.90$), resulting in a relatively large parallax error (2.08 mas). Our value of $\pi_{\rm trig} = 123.11 \pm 2.08$ mas places the star comfortably within 10 pc, and URAT's $\pi_{\rm trig} = 112.1 \pm 3.4$ mas supports the new 10 pc membership.
6. *0237−5928*: *APM 0237-5928* was reported in Henry et al. (2006) to have $\pi_{\rm trig} = 103.72 \pm 1.12$ mas, placing it near the 10 pc horizon. With a data set that now stretches nearly three times longer (18.1 years), we find $\pi_{\rm trig} = 99.75 \pm 0.85$ mas, placing the system just beyond 10 pc.
7. *0253+1652*: *SO 0253+1652* was discovered by Teegarden et al. (2003) as a potential nearby star of very high proper motion with $\mu = 5\farcs1$ yr$^{-1}$ and $\pi_{\rm trig} = 410 \pm 90$ mas (2.4 pc). We reported the first accurate parallax of $260.63 \pm 2.69$ mas in Henry et al. (2006) using 2.4 years of astrometry data, which was confirmed by Gatewood and Coban (2009), who found $\pi_{\rm trig} = 259.25 \pm 0.94$ mas. Here we update our parallax to $\pi_{\rm trig} = 261.01 \pm 1.76$ mas (3.8 pc) using 12.3 years of data. The system currently ranks as the 25th closest to the Sun.
8. *0301−1635*: *LTT 01445 ABC (LP 771-095 and LP 771-096 AB)* is a nearby triple first reported to be within 10 pc in Henry et al. (2006), with $\pi_{\rm trig} = 146.39 \pm 2.92$ mas for A and $139.70 \pm 4.99$ mas for BC based on 6.3 years of data. The BC pair is separated by $1\farcs3$ and is $7''$ from A. Astrometric residuals for A show the pull by the BC pair shown in Figure 2, and this trend has been removed in the reported parallax. We detect orbital motion in the BC pair, and an orbital fit with long period has been used to reduce the trend in the residuals, but the fit is not yet reliable. After 18.2 years of data, the parallaxes are consistent and the errors have been cut roughly in half, to $143.85 \pm 1.59$ mas for A and $142.57 \pm 2.03$ mas for BC.
9. *0335−4430*: *GJ 1061* was found to be the 20th nearest stellar system in Henry et al. (1997), with $\pi_{\rm trig} = 273.4 \pm 5.2$ mas determined using photographic plate data from Ianna's astrometry program in Siding Spring, Australia. Using the CCD camera on the 0.9 m, in Henry et al. (2006) we reported a parallax of $271.92 \pm 1.34$ using 6.3 years of data, and we update that value here to $270.53 \pm 1.18$ mas, with a data set now spanning 16.4 years. GJ 1061 currently ranks as the 22nd nearest system, given the addition of the closer brown dwarf systems WIS 0855-0714 and WIS 1049-5319 AB, but remains the 20th nearest stellar system and the nearest star discovered since YPC and *Hipparcos*. The star shows clear variability in the *V* band indicative of a stellar cycle, as well as a possible long-term trend, as shown in Figure 3.
10. *0339−3525*: *LP 944-020* has been a member of the 10 pc sample since the first parallax determination of $201.4 \pm 4.2$ mas by Tinney (1996), based on less than 2 years of data. Our published value of $155.89 \pm 1.03$ mas (Dieterich et al. 2014) is from 9.0 years of astrometric data and differs by $11\sigma$ from the earlier value. We update the value here to $156.33 \pm 0.78$ mas using 14.0 years of data. Although LP 944-020 is not a member of the 5 pc sample, it remains well within 10 pc.
11. *0352+1701*: *LHS 1610 AB* had a parallax of $70.0 \pm 13.8$ mas in the YPC, and we placed the system within 10 pc with a value of $101.57 \pm 2.07$ mas in Henry et al. (2006). Bonfils et al. (2013) reported the star to be an SB2, but the detailed study by Winters et al. (2018) indicates the system to be an SB1 with orbital period of 10.6 days and that the secondary is likely a brown dwarf. Our photometric distance estimate of $9.5 \pm 1.5$ pc is consistent with the trigonometric distance of 9.9 pc, indicating that the companion contributes minimal flux to the system. The system shows a decline in brightness in the *V* band of ∼10% from 2000 to 2010, and may be growing brighter since, as shown in Figure 3.
12. *0504+1103*: *LTT 17736 (G 097-015)* was estimated to be at a distance of 11.5 pc photometrically by Weis (1986). We measure a relative $\pi_{\rm trig} = 99.49 \pm 0.90$ mas, but the reference field is reddened with a correction of $4.07 \pm 0.42$ mas. We adopt a generic correction of $1.50 \pm 0.50$ mas, yielding an absolute $\pi_{\rm trig} = 100.99 \pm$

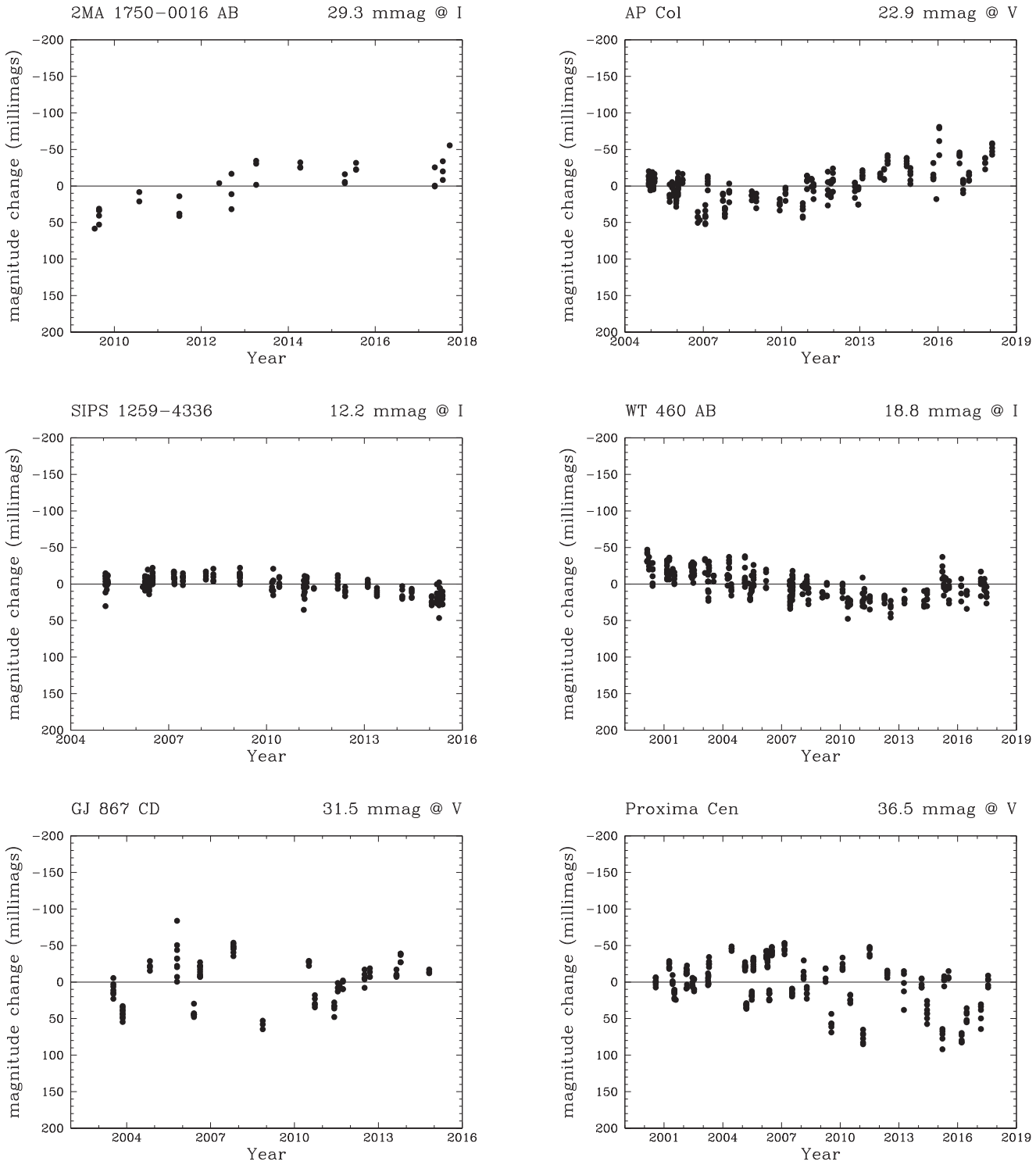


**Figure 4.** In the top four panels, photometric variability levels from 0.9 m data are shown for stars with trends in brightness that are likely portions of cycles longer than the durations of the current data sets. Points represent brightnesses in single frames and are shown oriented so that a star moves up on the plot when it grows brighter. Star names, variability measurements, and the filters used for the observations are given at the top of each panel. The cycles are longer than 8 years for 2MA 1750-0016 AB, 13 years for AP Col, 10 years for SIPS 1259-4336, and 17 years for WT 460 AB. The bottom two panels show the two most extreme variability measurements among the 75 systems in this paper. These stars appear to be highly spotted, with large, rapid changes in brightness. GJ 867 CD is a close binary, with an orbital period of 1.8 days where components incite activity in one another. The closest star, Proxima Centauri, shows variations of more than 10% in *V* during the 17 years of coverage.

1.03 mas, resulting in a distance just inside the 10 pc horizon.

13. *0528+0938*: *GJ 203* was a member of the 10 pc sample after results from YPC and *Hipparcos*, which resulted in a weighted mean of $\pi_{\rm trig} = 102.60 \pm 2.09$ mas. However, Dittmann et al. (2014) published $\pi_{\rm trig} = 92.9 \pm 2.5$ mas, reducing the weighted mean to $98.61 \pm 1.60$ mas. Our value of $\pi_{\rm trig} = 104.76 \pm 1.52$ mas brings the star back

into the 10 pc sample with a weighted mean of $\pi_{\rm trig} = 101.85 \pm 1.10$ mas.

14. *0604−3433*: *AP COL* was observed by RECONS starting in 2004 based upon our photometric distance estimate placing it at 4.6 pc. Soon thereafter, Scholz et al. (2005) placed the star (as LP 949-015) at a distance of 6.1 pc and noted it to be an active M dwarf. In 2011, we reported $\pi_{\rm trig} = 119.21 \pm 0.98$ mas using 6.5 years of data, placing the M4.5 star at a distance of 8.4 pc. The star's overluminosity on the HR diagram of Figure 5 is attributed to youth, supported by its photometric variability, lithium equivalent width, and gravity indicators (Riedel et al. 2011). It is therefore the nearest pre-main sequence star, and kinematics indicate that it is a likely member of the ∼40 Myr Argus/IC 2391 Association. We revise the parallax to 116.41 ± 0.81 mas (8.6 pc) here, and the 13.2 years of data also reveal a long-term change in brightness shown in Figure 4, indicative of a cycle lasting longer than the current data set.
15. *0630−7643*: *SCR 0630-7643 AB* is a new binary discovered during our SCR search (Hambly et al. 2004) and was first estimated photometrically to lie at 7.0 pc (Henry et al. 2004). The first $\pi_{\rm trig} = 114.16 \pm 1.85$ mas from Henry et al. (2006) was based on only 2.0 years of data, and is virtually unchanged here at $\pi_{\rm trig} = 114.11 \pm 1.44$ mas using 13.1 years of data. Significant orbital motion is seen, with the B component moving relative to A from 1.″97 at 22° on UT 2004 December 23 to 2.″66 at 78° on UT 2015 December 16, implying an orbital period on the order of 70 years. The astrometric reduction was done using frames with seeing greater than ∼1.″2, when the two components merged into a single source for centroiding.
16. *0717−0501*: *SCR 0717-0501* was first reported in Subasavage et al. (2005) as a new high-proper-motion star at an estimated distance of 15.9 pc based on SuperCOSMOS plate magnitudes combined with 2MASS. Finch and Zacharias (2016) reported a parallax of 104.60 ± 7.90 mas, but our value here of 92.86 ± 1.61 mas (a slight update to the value in Winters et al. 2017), places the system beyond 10 pc.
17. *0720−0846*: *WIS 0720-0846 AB* was revealed to be a likely nearby star by Scholz (2014) at an estimated distance of 7.0 pc via a parallax of 142 ± 38 mas. Burgasser et al. (2015) provided a second estimate of the distance via $\pi_{\rm trig} = 166 \pm 28$ mas and evidence that the system has a brown dwarf companion. We confirm a secondary that causes the large perturbation shown in Figure 2; once removed, we measure $\pi_{\rm trig} = 148.80 \pm 1.08$ mas (6.7 pc) using 4.0 years of data. With the relatively short time coverage, we can only say that the period is long, but the similar trigonometric and photocentric distances indicate that the secondary contributes minimal light to the system, consistent with it being of lower mass than the M9.0V primary (i.e., likely a brown dwarf). With $\mu = 109$ mas yr$^{-1}$, this is one of four new systems reported here with proper motions less than 200 mas yr$^{-1}$, ranking as the second slowest-moving system known within 10 pc. The star has been identified as possibly disrupting the Sun's Oort Cloud ∼70,000 years ago (Mamajek et al. 2015).
18. *0736+0704*: *LTT 17993 AB (G 089-032 AB)* was first reported to be a close double by Henry et al. (1999) with a separation of 0.″7 using infrared speckle imaging. The system was reported to have $\pi_{\rm trig} = 116.60 \pm 0.97$ mas using 6.1 years of data in Henry et al. (2006), and no perturbation was detected at that time. FWHM measurements of the system at the 0.9 m from 2000 to 2010 were always ∼1.″5, but steadily dropped to 1.″0 by 2018, implying a decreasing separation, and a long-term perturbation is now seen. A tentative orbital fit to residuals on both R.A. and decl. axes implies a period longer than the 18.0 years of available data, and that signal has been removed for the parallax of 117.59 ± 0.83 mas in Table 1. This is a promising system for accurate mass determinations.
19. *0740−4257*: *SCR 0740-4257* was first reported in (Subasavage et al. 2005), in which we estimated the distance to be 10.0 pc using SuperCOSMOS *BRI* plate magnitudes combined with 2MASS *JHK*. We then obtained accurate *VRI* magnitudes, and when combined with 2MASS estimated a distance of only 7.2 pc in Winters et al. (2011). Here we present the first parallax, $\pi_{\rm trig} = 127.71 \pm 0.76$ mas, based on 11.1 years of data, placing the system at 7.8 pc. This is supported by a URAT value of $\pi_{\rm trig} = 122.7 \pm 4.0$ mas. As shown in Figure 3, the star appears to show a low-level photometric variation in *R* with period of ∼7 years.
20. *0751−0000*: *GJ 1103 (LHS 1951)* was reported in Luyten (1979) to have a companion 3″ from the M4.5V star. Our own monitoring at the 0.9 m from 2004 to 2018 in the *V* filter does not reveal any companion at that separation, nor to separations as small as the seeing, 0.″9 in the best frames. In addition, we find no perturbation on the position of the photocenter after solving for parallax and proper motion over 13.1 years of monitoring. Blinking of plate images reveals a background star as the "B" component at that separation and position angle in POSS-I plates from 1953, so we conclude that the reported "companion" is a background star.
21. *0815−2344*: *UPM 0815-2344 AB* is the first system from the USNO Proper Motion (UPM) survey by Finch et al. (2014) confirmed to be within 10 pc via a RECONS parallax measurement, $\pi_{\rm trig} = 105.05 \pm 0.87$ mas (9.5 pc) reported here. This distance is consistent with their photometric distance estimate of 11.1 ± 2.6 pc, and is confirmed by a URAT parallax of 102.9 ± 3.4 mas. The B component creates a slight tail in the isophotal contour plot, about 1.″5 from the primary; no orbital motion nor perturbation is yet seen in the 3.2 years of data. With $\mu = 138$ mas yr$^{-1}$, this is one of four new systems reported here with proper motions less than 200 mas yr$^{-1}$, ranking fifth among all systems within 10 pc.
22. *0818−6818*: *L 098-059* slips into the 10 pc sample with $\pi_{\rm trig} = 101.81 \pm 2.37$ mas. The error is large because of a relatively faint field of reference stars compared to the $R = 10.61$ star.
23. *0835−0819*: *2MA 0835-0819* has a $\pi_{\rm trig} = 117.3 \pm 11.2$ mas (8.5 pc) in Andrei et al. (2011), but the error was too large for inclusion in the 10 pc sample. Parallaxes by Weinberger et al. (2016; 137.49 ± 0.39), Dahn et al. (2017; 138.71 ± 0.58 mas), and our value here (138.33 ±; 0.93 mas) are all virtually identical and place

this brown dwarf within 10 pc, and substantially closer (7.2 pc) than the original distance.

24. *0858+0828*: *LTT 12352 ABC (G 041-014 ABC)* is a close triple in which all three components are separated by less than 1″, as discussed in Henry et al. (2006). The five reference stars are faint, and with an average integration time of only 37 s the astrometric residuals are relatively high. Nonetheless, even after 18.0 years, no perturbation is seen, and images have FWHM as small as 1.″0 with no obvious elongation.
25. *0915−1035*: *LHS 6167 AB* was identified as a possible nearby star by Finch & Zacharias (2016) with $\pi_{\rm trig} = 134.9 \pm 12.1$ mas, although the large parallax error precluded its entry into the 10 pc sample. A parallax of $103.30 \pm 1.00$ mas using 9.3 years of data was reported in Bartlett et al. (2017), adding the system to the sample. The binary has been resolved several times, always at a separation less than 0.″2 (see Bartlett et al. 2017, Table 9). We provide an updated parallax value of $\pi_{\rm trig} = 103.54 \pm 0.77$ mas based on 13.3 years of data that includes the orbital fit (see Table 2) with period of 4.8 years shown in Figure 1. The system flared by 0.25 mag in the *V* band on UT 2013 April 02.
26. *1048−3956*: *DEN 1048-3956* was targeted by RECONS in both our 0.9 m and 1.5 m astrometry programs, yielding parallaxes of $247.71 \pm 1.55$ mas (Jao et al. 2005) and $249.78 \pm 1.81$ mas (Costa et al. 2005), respectively. The 0.9 m result was updated in Lurie et al. (2014) to $\pi_{\rm trig} = 248.08 \pm 0.61$ mas, where orbiting planets with masses of 1–2 Jupiters were eliminated for periods of 2–12 years. Now with 14.9 years of data, we adjust the parallax slightly to $\pi_{\rm trig} = 247.78 \pm 0.60$ mas, which now ranks this M8.5V star as the 30th nearest system to the Sun.
27. *1141−3624*: *SIPS 1141-3624* was first reported in Deacon et al. (2005a) as part of a survey for new high proper motion stars using a combination of data from the SuperCOSMOS sky survey and 2MASS. We estimate the distance photometrically to be 9.9 pc, whereas our $\pi_{\rm trig} = 116.12 \pm 1.30$ mas is the first, corresponding to 8.6 pc. A URAT value of $\pi_{\rm trig} = 107.1 \pm 4.7$ mas confirms the systems's proximity. The star appears to exhibit a low amplitude photometric cycle in the *R* band of duration ∼7 years.
28. *1155−3727*: *2MA 1155-3727* is an object near the stellar/substellar border reported to have $\pi_{\rm trig} = 104.40 \pm 4.70$ mas in Faherty et al. (2012). Values from both Weinberger et al. (2016; $\pi_{\rm trig} = 84.36 \pm 0.85$ mas) and our value here ($\pi_{\rm trig} = 82.76 \pm 1.74$ mas) place this object well beyond 10 pc.
29. *1159−5247*: *1RXS 1159-5247* was put on the 0.9 m program in 2009, given our photometric distance estimate of 10.6 pc. Sahlmann et al. (2014) reported a parallax of $\pi_{\rm trig} = 105.54 \pm 0.12$ mas for the star, which was part of an astrometric search for planets around 20 nearby stars. We measure $\pi_{\rm trig} = 106.25 \pm 0.69$ mas, consistent with the Sahlmann et al. (2014) value.
30. *1214+0037*: *GJ 1154* was reported to be an unresolved SB2 by Bonfils et al. (2013), with variable spectral-line width. We detect no perturbation in 4.8 years of data, and the value of $\pi_{\rm trig} = 124.68 \pm 1.83$ mas yields a distance of $8.0 \pm 0.1$ pc that is marginally consistent with the photometric distance of $6.3 \pm 1.0$ pc. Although the distance offset may indicate flux contributed by an unseen secondary, we await confirmation of the companion before listing the system as a close double.
31. *1259−4336*: *SIPS 1259-4336* is a high proper motion star ($\mu = 1.''145\ {\rm yr}^{-1}$) first reported in Deacon et al. (2005a) to be at a distance of only 3.6 pc based on $\pi_{\rm trig} = 276 \pm 41$ mas. We estimate the distance to be 8.1 pc photometrically, and determine a distance of 7.8 pc from $\pi_{\rm trig} = 127.93 \pm 0.50$ mas, more than twice as distant as the initial parallax estimate. The low formal error is representative of our very best parallaxes. A slight long-term trend in brightness over a decade in the *I* band is evident, as shown in Figure 4.
32. *1411−4132*: *WT 460 AB* entered the 10 pc sample after our first determination of $\pi_{\rm trig} = 107.41 \pm 1.52$ mas (Henry et al. 2006). A low mass companion was first reported by Montagnier et al. (2006) at a separation of 0.″51 mas and brightness difference in the *H* band of 2.47 mag. The companion causes a large perturbation shown in Figure 2 that we remove to derive an updated parallax of $108.53 \pm 0.74$ mas using 17.3 years of data. The photocentric shifts are 250 mas in both R.A. and decl. and show no sign of abating, implying a period of at least several decades. As shown in Figure 4, this system has been found to exhibit a long-term photometric trend in the *I* band, with the flux dropping ∼5% from 2000 to 2012, followed by a turnaround in the past few years.
33. *1416+1348*: *SDSS 1416+1348 AB* is a brown dwarf pair separated by 9″ for which the first parallax of $109.7 \pm 1.3$ mas was published by Dupuy & Liu (2012). Our value of $106.77 \pm 1.24$ mas derived after 7.0 years of data is consistent, and secures this double brown dwarf as one of only four known within 10 pc.
34. *1429−6240*: *PROXIMA CENTAURI* We have observed the nearest star to the Sun for 17.0 years and measure a parallax of $769.66 \pm 0.83$ mas, consistent with the weighted mean of $768.74 \pm 0.30$ mas from YPC, *Hipparcos*, and *HST* (Benedict et al. 1999). Proxima is undoubtedly a highly spotted star, with variations of more than 10% in the *V* band, as shown in Figure 4. In fact, its measured variability of 36.5 mmag is the largest for any star among the 75 discussed in this paper. A rotation period of ∼83 days has been derived for Proxima (Benedict et al. 1998) and the star has been known to flare (e.g., MacGregor et al. 2018), although we have not observed a major flare during our observations.
35. *1540−5101*: *WIS 1540-5101* is a high proper motion M dwarf with $\mu = 1.''981\ {\rm yr}^{-1}$ that had two crude parallax measurements of $228 \pm 24$ mas (Pérez Garrido et al. 2014) and $165 \pm 41$ (Kirkpatrick et al. 2014). Our photometric distance estimate of 5.1 pc is consistent with our $\pi_{\rm trig}$ 187.93 = ± 1.15 mas (5.3 pc). The measurement is based on only 2.0 years of data, although we deem the result reliable because we have sampled the extrema of the parallax ellipse, and reductions with earlier frame sets are consistent with the value presented here.
36. *1542−1928*: *GJ 595 AB* has long been known to be nearly 10 pc away, with $\pi_{\rm trig} = 99.42 \pm 3.46$ mas from the weighted mean parallaxes of YPC

(101.60 = ± 4.40 mas) and *Hipparcos* (95.50 = ± 5.59 mas) values. At $V = 11.84$, this is near the faint limit of *Hipparcos*, so the $\pi_{\rm trig}$ error was relatively large. Nidever et al. (2002) discovered a companion with orbital period 63 days and minimum mass 60 $M_{\rm Jup}$ that may have confounded previous parallax efforts. We confirm the companion in our astrometry data using 5.4 years of data, and derive a nearly edge-on orbit (see Table 2) with a period of 62.0 ± 0.1 days and photocentric semimajor axis of 9 mas. The inclination of 95° implies that the companion is a brown dwarf. After fitting the orbit shown in Figure 1, we measure $\pi_{\rm trig} = 108.02 \pm 1.31$ mas, placing the system comfortably within 10 pc.

37. *1546−5534*: *SCR 1546-5534 AB* was discovered by the RECONS team (Boyd et al. 2011), where we estimated the distance to be 6.7 pc using SuperCOSMOS *BRI* plate magnitudes combined with 2MASS *JHK*. Combining accurate *VRI* (Winters et al. 2011) with 2MASS, we derived an identical photometric distance estimate of 6.7 pc. With 6.1 years of astrometric data, we now see a clear perturbation shown in Figure 2 caused by a companion unseen in our images. The perturbation is quite large with photocenter shifts of ∼100 mas in both R.A. and decl., and the orbit has not clearly wrapped. Removal of the perturbation results in a relative $\pi_{\rm trig} = 103.11 \pm 0.87$ mas, placing the system near 10 pc. The reference stars yield a correction to absolute parallax of 3.42 mas, so we have adopted a generic correction of 1.50 ± 0.50 mas. The offset between the trigonometric and photocentric distances indicates that the secondary contributes significant light to the system and is not of low mass, consistent with the large perturbation.
38. *1645−1319*: *2MA 1645-1319* was reported in Faherty et al. (2012) to have $\pi_{\rm trig} = 109.9 \pm 6.1$ mas, but our value of 90.12 ± 0.82 mas from Dieterich et al. 2014 using 4.0 years of data indicates that this star is not within 10 pc. We provide a slightly revised value of 90.89 ± 0.80 mas based on more than twice as much data (8.2 years).
39. *1731+2721*: *2MA 1731+2721* was reported to have $\pi_{\rm trig} = 113.8 \pm 7.0$ mas in Dittmann et al. (2014), but here we find $\pi_{\rm trig} = 85.54 \pm 1.69$ mas based on 6.2 years of data, placing the star well beyond 10 pc.
40. *1737−4419*: *GJ 682* has a weighted mean parallax of 199.65 ± 2.30 mas from YPC and *Hipparcos*, placing it just beyond 5 pc. During observations spanning 14.0 years, the target star moves in front of a few background stars, but we deem our $\pi_{\rm trig} = 203.49 \pm 1.30$ mas value reliable, indicating that the star is a new addition to the 5 pc sample. A generic correction of 1.50 ± 0.50 mas from relative to absolute parallax has been used because the background stars are reddened.
41. *1750−0016*: *2MA 1750-0016 AB* is a brown dwarf reported by Andrei et al. (2011) to have $\pi_{\rm trig} = 108.5 \pm 2.6$ mas. Dahn et al. (2017) confirmed its proximity via a parallax of 110.59 ± 0.52 mas. We have discovered an unseen companion, presumably a lower mass brown dwarf, that causes the perturbation on the photocenter shown in Figure 1. An orbital fit to the motion (see Table 2) yields a period of 6.7 years and semimajor axis of 13 mas, and once removed, we find a parallax of 111.47 ± 1.18 mas (9.0 pc). This is the fourth binary brown dwarf known within 10 pc and the third closest, along with WIS 1049-5319 AB (2.0 pc), ϵ Indi BC (3.6 pc), and SDSS 1416+1348 AB (9.1 pc). As shown in Figure 4, the system also shows a trend in flux, growing brighter in the *I* band by ∼6% over 8 years.
42. *1843−5436*: *LHS 5341* is a virtually unexplored single red dwarf for which we measure $\pi_{\rm trig} = 101.57 \pm 1.01$ mas, placing the star at 9.8 pc. A URAT value of $\pi_{\rm trig} = 105.9 \pm 5.5$ mas supports its membership in the 10 pc sample. This is a classic case of a nearby star in the southern sky, about which almost nothing is known; the only previous study of this star is our own, indicating that it is not variable by 20 mmag over ∼6 years in the *R* band (Hosey et al. 2015).
43. *1845−6357*: *SCR 1845-6357 AB* is the nearest star discovered via the SuperCOSMOS-RECONS effort. The primary is an M8.5V star first reported in Hambly et al. (2004), with a brown dwarf secondary first imaged by Biller et al. (2006) at a separation of 1.″17. We published the first parallax estimate in Deacon et al. (2005b), $\pi_{\rm trig} = 282 \pm 23$ mas, using scans of eight SuperCOSMOS scans of plates in the UK Schmidt Telescope Unit plate library. We followed this with a measurement from the 0.9 m program in Henry et al. (2006), determining $\pi_{\rm trig} = 259.45 \pm 1.11$ mas. Here we provide an updated value that is significantly smaller, at 251.27 ± 0.54 mas. The parallax has changed because of the slow orbital pull by the brown dwarf companion that affected the initial parallax value determined using only 2.6 years of data. The value presented here uses 14.5 years of data for which the perturbation shown in Figure 2 has been fit and removed. The orbital period is likely a century or more, so the fit is certainly not the true orbit, but it does improve the parallax measurement. At 4.0 pc, the system currently ranks as the 28th nearest.
44. *2049−4012*: *SCR 2049-4012 AB* has an estimated photometric distance of 8.0 pc, which is closer than the 9.6 pc result from the parallax $\pi_{\rm trig} = 104.39 \pm 0.87$ mas. URAT provides an additional measurement of $\pi_{\rm trig} = 107.6 \pm 4.4$ mas, confirming that the system is within 10 pc. The offset between the photometric and trigonometric distances is likely due to the unseen companion causing the perturbation with orbital period of ∼1.8 years shown in Figure 1, although the other orbital elements (see Table 2) are likely unreliable. With $\mu = 68$ mas yr$^{-1}$, this is one of four new systems reported here with proper motions less than 200 mas yr$^{-1}$, and ranks as the slowest-moving system known within 10 pc.
45. *2050−3424*: *2MA 2050-3424* is from the southern SUPERBLINK survey, reported in Lépine (2008). Our photometric distance estimate of 9.5 pc is consistent with the $\pi_{\rm trig} = 105.61 \pm 1.10$ mas (9.5 pc) RECONS measurement. URAT also finds a value that places the star within 10 pc, $\pi_{\rm trig} = 101.0 \pm 5.6$ mas.
46. *2238−2036*: *GJ 867 CD* is part of a quadruple system, composed of two close doubles, AB and CD,[13] separated by 24″, corresponding to a projected separation of

[13] Here we describe the system as AB–CD rather than AC–BD, as used by Davison et al. (2014); we have reassigned the nomenclature to be consistent with the likely order of brightness at *V*.

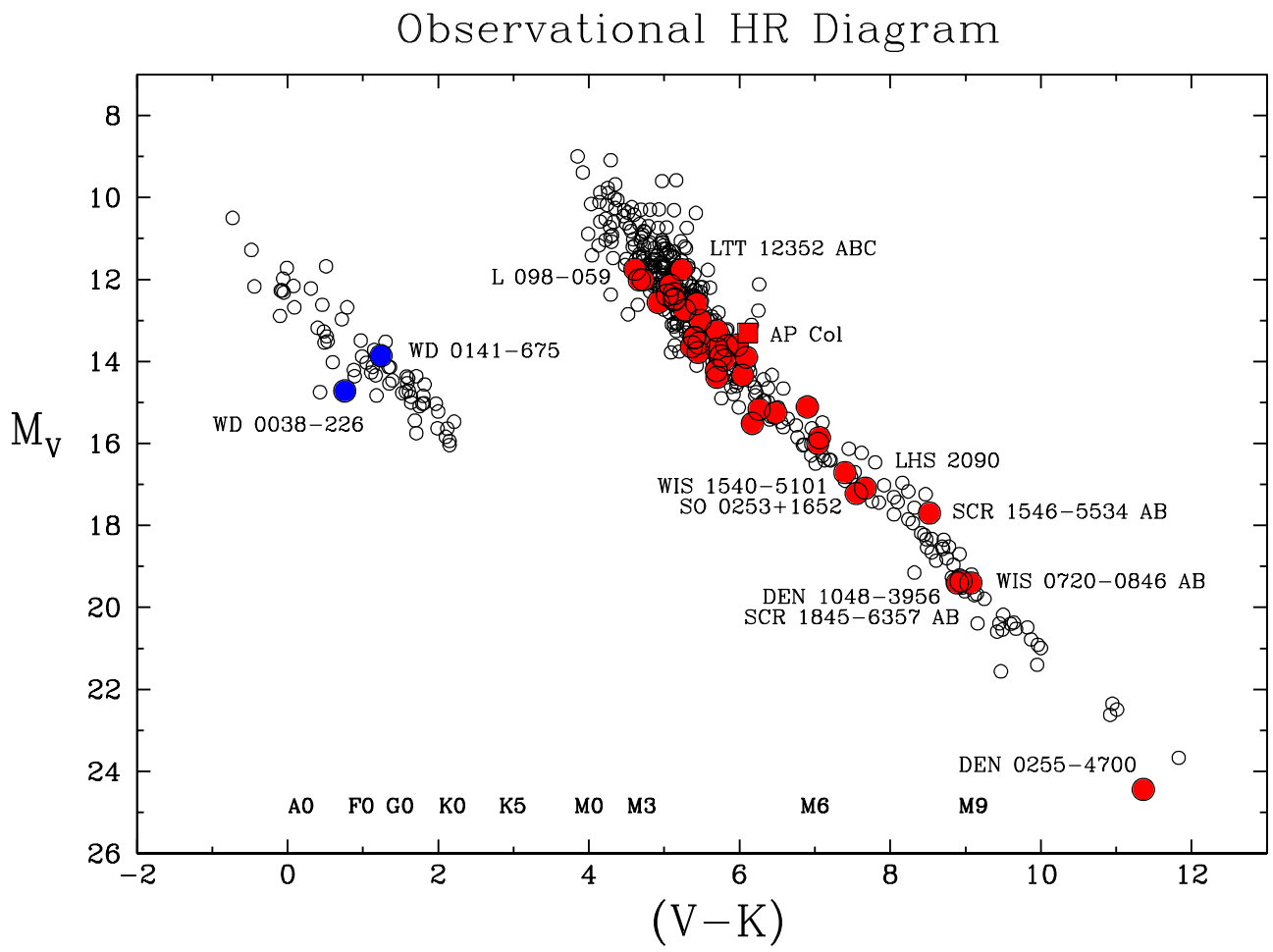


**Figure 5.** An observational HR diagram is shown for systems within 25 pc determined via trigonometric parallaxes from the CTIO/SMARTS 0.9 m. Included are the 42 red and brown dwarf systems (red points) and two white dwarfs found within 10 pc by RECONS (blue points). The single solid square point represents the pre-main sequence star AP Col, which is only 8.6 pc away. Open black circles are additional measurements of targets within 25 pc. The two brightest systems are labeled, as well as the eight intrinsically faintest, reddest systems.

~200 au. The AB pair exhibits an SB2 orbital period of 4.08 days, $K_1 = 46.8\,\mathrm{km\,s^{-1}}$, and $K_2 = 58.1\,\mathrm{km\,s^{-1}}$ (elements from Herbig & Moorhead 1965). Davison et al. (2014) found the fourth component via radial velocity monitoring of the C component, determining an SB1 orbit with a period of 1.80 days and $K_1 = 21.4\,\mathrm{km\,s^{-1}}$. At such a short period, our astrometry of CD reveals no perturbation, but the proximity of the components likely causes the high level of photometric variability shown in Figure 4. The new D component remains to be imaged, but the minimum mass is $0.056\,M_\odot$, so it is either a high-mass brown dwarf or M star.

47. *2248−2422*: *LP 876-010* is the tertiary in the triple system containing Fomalhaut (A), GJ 879 (B, also known as TW PsA), and LP 876-010 (C). LP 876-010 is listed in the middle portion of Table 1 because A and B were previously known to be within 10 pc, although the C component was not. The system was thoroughly discussed in Mamajek et al. (2013), where the C component was identified as part of the system. The $\pi_{\rm trig}$ in that paper for C (132.07 ± 1.19 mas) is updated here to 132.27 ± 1.07 mas using 10.4 years of data. This value is consistent with the values of 129.81 ± 0.47 mas for A and 131.42 ± 0.62 mas for B (van Leeuwen 2007).

## 6. Discussion

### 6.1. The HR Diagram

Figure 5 illustrates an observational HR diagram for stars within 25 pc having parallaxes measured during the RECONS program at the 0.9 m, for which a complete list of results can be found at www.recons.org. We use $M_V$ versus $V-K$ as proxies for the luminosities and temperatures of targets.

Solid red points represent red and brown dwarfs for which RECONS has published the first accurate parallax for the system placing it within 10 pc. Solid blue points represent the two white dwarfs added to the 10 pc sample. Open circles represent additional stars within 25 pc, for which $\pi_{\rm trig}$ was measured at the 0.9 m. These are primarily red dwarfs, published in several previous papers in this series (Jao et al. 2005, 2011, 2014, 2017; Henry et al. 2006; Riedel et al. 2010, 2014; Mamajek et al. 2013; Dieterich et al. 2014; Lurie et al. 2014; Davison et al. 2015; Benedict et al. 2016; Bartlett et al. 2017; Winters et al. 2017), and in two papers reporting parallaxes for white dwarfs (Subasavage et al. 2009, 2017).

The new 10 pc systems stretch from L 098-059 and the triple LTT 12352 ABC with $M_V = 11.8$ and types M2.5V–M3.5V, to the three faintest, DEN 1048-3956, SCR 1845-6357 AB, and WIS 0720-0846 AB with $M_V = 19.4$ and types M8.5V–M9.5V. The single brown dwarf, DEN 0255-4700, at the

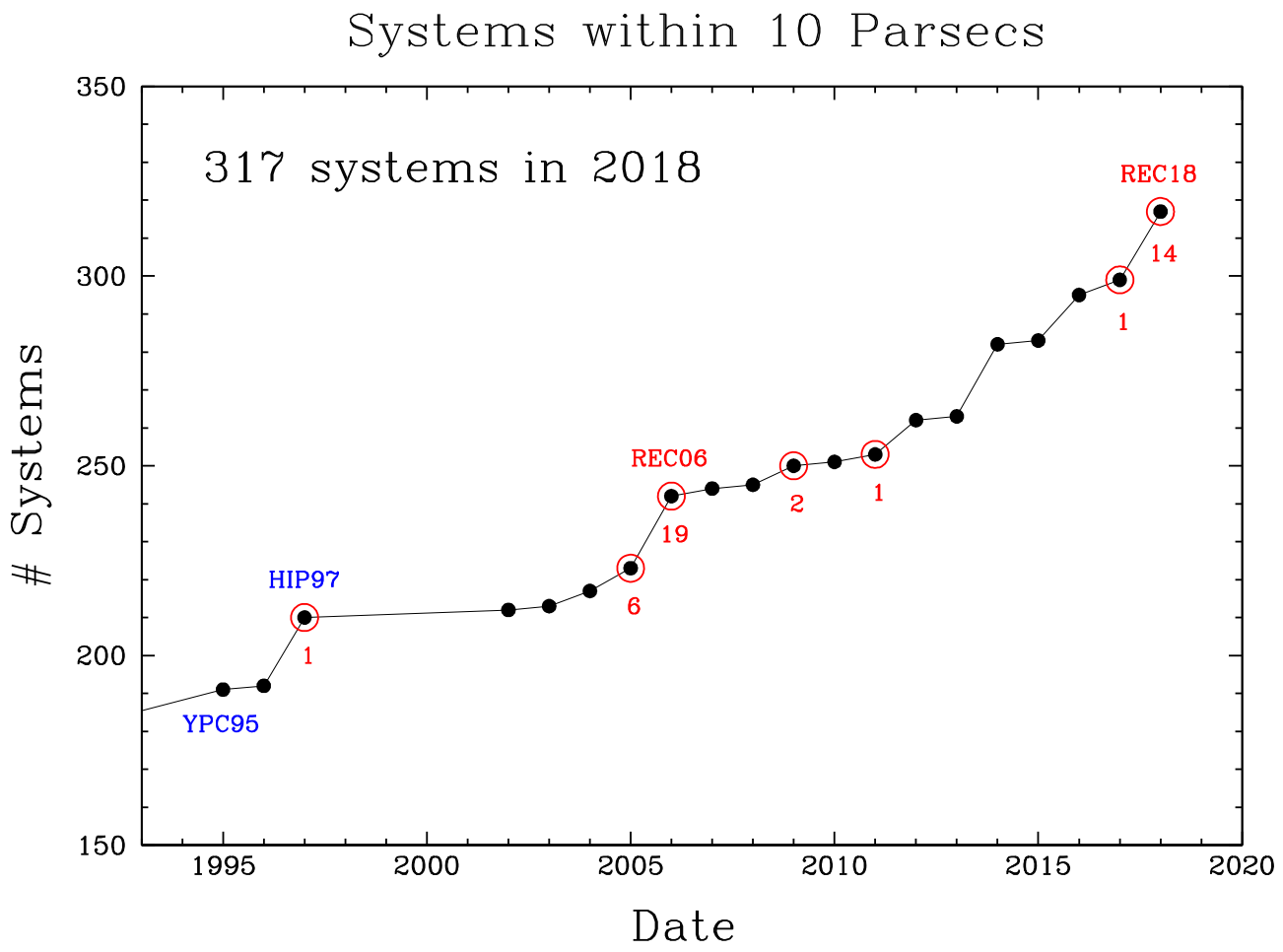


**Figure 6.** The growth of the 10 pc sample is shown from the publication of the Yale Parallax Catalog in 1995 (the YPC95 point) to the present. *Hipparcos* contributed 17 systems in 1997, as indicated with the label HIP97. At least one system has been added to the sample every year starting in 2002, and the census has steadily risen since. Points encircled with red are years in which RECONS added the number of systems indicated with red digits. REC06—Henry et al. (2006) and REC18—this paper.

lower right of the plot has $M_V = 24.4$. The pre-main sequence star AP Col at 8.6 pc (Riedel et al. 2011), shown with a red square, is clearly elevated above the main sequence red dwarfs. In all, 27 of the systems have $V - K = 5.0$–$7.0$, typical of the red dwarf population that is rich in spectral types M3.0V–M5.0V. Among the nine faintest, reddest star systems having $V - K = 7.0$–$9.1$, there are five close multiples that are excellent targets for mass determinations.

### 6.2. Evolution of the 10 pc Sample

Figure 6 charts the total number of systems in the 10 pc sample over the past two decades, since the publication of the YPC in 1995. These recent contributions to the 10 pc sample are listed in Table 4. Red numbers under various points indicate the 44 systems added by RECONS to the sample. After a 5-year pause in nearby star parallaxes after the *Hipparcos* mission, the census has continued to climb steadily, with the additions of stars as well as systems composed only of brown dwarfs. Among the 317 systems known within 10 pc today, only 191 were identified and had parallaxes with errors less than 10 mas at the time of the YPC, indicating an overall increase of 66%. Since 1995, 126 systems have been added, including 6 FGK systems from *Hipparcos*, 3 white dwarfs, 79 red dwarf systems, and 38 brown dwarf systems. Thus, a total of 88 stellar systems have been added to the 10 pc sample, more than twice the number of brown dwarf-only systems. Notably, the rate of increase has yet to slow, although of course there will be a turnover in the census curve when all systems have been found. We predict that there will be a short list of stars contributed by *Gaia* soon (see Section 6.4).

Since the millennium, the RECONS group has focused its efforts on identifying red and white dwarfs missing from the nearby sample (Henry et al. 2003), and published its first parallaxes in 2005 (Costa et al. 2005; Jao et al. 2005), 10 years after the YPC. As outlined in Table 4, the largest number of systems added to the 10 pc census in the past two decades was the 18 systems added in Henry et al. (2006).[14] The second largest set of additions (17 systems) was from *Hipparcos* and the third (14 systems) is from this paper. After RECONS and *Hipparcos*, the largest contributions are the nine systems from the USNO program in Flagstaff (Dahn et al. 2002, 2017; Vrba et al. 2004) and the eight systems from URAT observations (Finch & Zacharias 2016; Finch et al. 2018), for which we provide confirming parallaxes for seven more systems here. As detailed in Table 4, some recent efforts have focused on using

[14] Two systems near the 10 pc border in that paper have now been found to be just further than 10 pc—APM 0237-5928 and LHS 1302—as discussed in Section 5.

**Table 4**
Systems Added to the 10 pc Census since 1995[a]

| Reference | Observing Method | Other[b] Dwarfs | Red[b] Dwarfs | Brown[b] Dwarfs | Total Systems | New 10 pc Systems |
|---|---|---|---|---|---|---|
| | | New Systems within 10 pc from RECONS Parallax Efforts | | | | |
| Henry et al. (1997) | phot plates | 0 | 1 | 0 | 1 | GJ1061 |
| Costa et al. (2005) | optical CCD | 0 | 1 | 0 | 1 | GJ2005 |
| Jao et al. (2005) | optical CCD | 0 | 5 | 0 | 5 | GJ754 GJ1068 GJ1123 GJ1128 DEN1048-3956 |
| Costa et al. (2006) | optical CCD | 0 | 0 | 1 | 1 | DEN0255-4700 |
| Henry et al. (2006) | optical CCD | 0 | 18 | 0 | 18 | see Table 1 |
| Subasavage et al. (2009) | optical CCD | 2 | 0 | 0 | 2 | WD0038-226 WD0141-675 (2 white dwarf systems) |
| Riedel et al. (2011) | optical CCD | 0 | 1 | 0 | 1 | APCOL |
| Bartlett et al. (2017) | optical CCD | 0 | 1 | 0 | 1 | LHS6167 |
| this paper | optical CCD | 0 | 14 | 0 | 14 | see Table 1 |
| TOTAL from RECONS | | 2 | 41 | 1 | 44 | |
| | | New Systems within 10 pc from Other Parallax Efforts | | | | |
| Tinney (1996) | optical CCD | 0 | 1 | 0 | 1 | LP944-020 |
| ESA (1997) | *Hipparcos* | 6 | 11 | 0 | 17 | 2 F, 1 G, 3 K, 11 M star systems |
| Dahn et al. (2002) | optical CCD | 0 | 0 | 2 | 2 | 2MA0036+1821 2MA1507-1627 |
| Reid et al. (2003) | optical CCD | 0 | 1 | 0 | 1 | 2MA1835+3259 |
| Vrba et al. (2004) | IR array | 0 | 0 | 4 | 4 | 2MA0415-0935 2MA0727+1710 2MA0937+2931 2MA1217-0311 |
| van Leeuwen (2007) | *Hipparcos* | 0 | 2 | 0 | 2 | GJ569 L026-027 |
| Burgasser et al. (2008) | IR array | 0 | 0 | 1 | 1 | 2MA0939-2448 |
| Gatewood & Coban (2009) | optical CCD | 0 | 1 | 0 | 1 | LSPM0011+5908 |
| Lépine et al. (2009) | optical CCD | 0 | 2 | 0 | 2 | LSPM0330+5413 LSPM0510+2714 |
| Marocco et al. (2010) | IR array | 0 | 0 | 1 | 1 | CFB0059-0114 |
| Andrei et al. (2011) | optical CCD | 0 | 0 | 1 | 1 | 2MA1750-0016 |
| Dupuy & Liu (2012) | IR array | 0 | 0 | 2 | 2 | 2MA1503+2525 SDSS1416+1348 |
| Faherty et al. (2012) | optical CCD/IR array | 0 | 1 | 4 | 5 | 2MA0034+0523 2MA0439-2353 2MA0729-3954 2MA1114-2618 LEHPM1-3396 |
| Leggett et al. (2012) | IR array | 0 | 0 | 1 | 1 | UGPS0722-0540 |
| Shkolnik et al. (2012) | optical CCD | 0 | 1 | 0 | 1 | LP655-048 |
| Smart et al. (2013) | IR array | 0 | 0 | 1 | 1 | 2MA2139+0220 |
| Beichman et al. (2014) | various IR | 0 | 0 | 3 | 3 | WIS0410+1502 WIS1738+2732 WIS2056+1459 |
| Boffin et al. (2014) | optical CCD | 0 | 0 | 1 | 1 | WIS1049-5319 |
| Dittmann et al. (2014) | optical CCD | 0 | 7 | 0 | 7 | G141-036 LP071-082 LP355-032 LP502-056 LSPM2044+1517 LSPM2146+3813 LTT16843 |
| Sahlmann et al. (2014) | optical CCD | 0 | 1 | 0 | 1 | 1RXS1159-5247 |
| Tinney et al. (2014) | IR array | 0 | 0 | 6 | 6 | WIS0713-2917 WIS1141-3326 WIS1541-2250 WIS1639-6847 WIS2134-7137 WIS2325-4105 |
| Zapatero Osorio et al. (2014) | IR array | 0 | 0 | 1 | 1 | 2MA0355+1133 |
| Gizis et al. (2015) | optical CCD | 0 | 0 | 1 | 1 | 2MA2148+4003 |
| Faherty et al. (2016) | optical CCD | 0 | 0 | 1 | 1 | 2MA0652+4710 |
| Finch & Zacharias (2016) | optical CCD | 0 | 4 | 0 | 4 | 2MA2000+3057 G184-031 LTT11586 TYC3251-1875-1 |
| Luhman & Esplin (2016) | various space | 0 | 0 | 1 | 1 | WIS0855-0714 |
| Sahlmann et al. (2016) | optical CCD | 0 | 0 | 1 | 1 | 2MA1821+1414 |
| Weinberger et al. (2016) | optical CCD | 0 | 3 | 2 | 5 | 2MA0835-0819 GJ1028 SIM0136+0933 LP991-084 SIPS1259-4336 |
| Dahn et al. (2017) | optical CCD | 0 | 0 | 3 | 3 | WIS0607+2429 WIS1405+8350 2MA1515+4847 |
| Finch et al. (2018) | optical CCD | 1 | 3 | 0 | 4 | LHS2597 LHS5264 UCAC4-379-100760 UPM0812-3529 (+7 confirmations in this paper) |
| TOTAL from other programs | | 7 | 38 | 37 | 82 | |
| TOTAL from all programs | | 9 | 79 | 38 | 126 | |

**Notes.**
[a] Systems must have weighted mean trigonometric parallaxes of 100 mas or more and errors of 10 mas or less.
[b] Primaries are used to categorize systems as white, red, or brown dwarf additions.

infrared arrays to measure parallaxes for brown dwarfs,[15] particularly targeting new candidates from the *WISE* spacecraft. Noteworthy are the two remarkable discoveries of WIS 1049-5319 AB (2.0 pc) by Luhman (2013) and WIS 0855-0714 (2.2 pc) by Luhman (2014). In the latter case, the current best parallax was determined using only space-based platforms: *HST*, *Spitzer*, and *WISE* (Luhman & Esplin 2016). Nonetheless, somewhat surprising is the continuing utility of optical CCDs for measuring parallaxes to nearby systems.

### 6.3. Missing Systems

At this juncture in the RECONS effort to reveal nearby stars, it is instructive to revisit the estimate of "missing" systems outlined in Figure 1 of Henry et al. (1997). For this discussion, we focus on *stellar* systems, rather than brown dwarfs, given that no brown dwarf primaries were known in 1997 and they likely remain underrepresented in the present sample.[16] In 1997, there were 45 systems known within 5 pc, indicating that there should be 360 systems within 10 pc, assuming a constant space density. However, at the time, only 229 systems were known, implying that 131 systems (36%) were unaccounted for.

As of this writing, there have been four *stellar* systems[17] found within 5 pc since the discovery of GJ 1061 (20th nearest), the subject of the Henry et al. (1997) effort: SO 0253+1652 (23rd nearest), SCR 1845-6357 AB (26th nearest), DEN 1048-3956 (29th nearest), and LHS 288 (43rd nearest), all of which had their first high-quality parallaxes published by RECONS. There has also been a swap in membership since then, with LP 944-020 dismissed from the 5 pc sample and GJ 682 added here. Thus, the gain within 5 pc is four stellar systems, bringing the total to 49. Again assuming a constant density, this translates to 392 systems within 10 pc, while the current 10 pc list contains only 279 systems with stellar primaries. This implies that 113 systems (29%) are still missing.

Given only the slight drop from 36% incompleteness in 1997 to 29% in 2018, it seems that we have made only minor progress in completing the sample, but certainly a 22% increase (from 229 to 279 systems) in the number of verified stellar systems nearest to the Sun is a scientific advance. However, it is important to note that the standard deviation of our presumably Poisson sampling of the distribution of the 5 pc stellar population, $\sigma = N^{1/2}$, where $N = 49$ star systems, is $\pm 7$ systems. This corresponds to $\pm 56$ systems at 10 pc for eight times the volume. Thus, the difference between the observed (279 systems) and anticipated (392 systems) populations is only twice the standard deviation, indicating that our progress may be more significant than perceived if the 392 target systems is an overestimate. *Considering this numerical treatment and our experience in searching for nearby stars over 2 decades, we predict that the complete census of systems within 10 pc with stellar primaries will eventually be found to be ~300, indicating that the sample is currently at least 90% complete.*

### 6.4. Gaia *Data Releases*

On September 14, 2016, the first astrometry data from *Gaia* were provided via Data Release 1 (DR1), including parallaxes for ~2 million stars observed by Tycho, the auxiliary star mapper on the *Hipparcos* spacecraft. However, Jao et al. (2016) found small but systematic offsets between *Gaia* and *Hipparcos* parallaxes in a study of 612 stars within 25 pc. In addition, a careful evaluation of the *Gaia* DR1 results indicates that there would be very few changes to the sample. Of the 62 systems in the 10 pc list in *Gaia* DR1, four—GJ 239, GJ 678.1, L 026-027, and L 098-059—would slip beyond 10 pc, and none by more than a few mas. In balance, three new entries would occur—GJ 172, GJ 436, and TYC 3980-1081-1. The latter star is the only one for which the parallax ($120.59 \pm 0.96$ mas) places it well within 10 pc. This star was previously identified as a possible nearby star by Finch & Zacharias (2016) with $\pi_{\rm trig} = 154.8 \pm 12.1$ mas, although because of the large error, it was not yet in the sample.

In sum, *Gaia* DR1 data change the character of the 10 pc sample very little, and all of the parallaxes used to determine membership in the sample are likely to change somewhat in the soon-to-be-released *Gaia* DR2 results. Thus, instead of incorporating the initial DR1 results, we await the DR2 results that are based upon a greater timespan of data, and when the data set extends to fainter magnitudes. Ultimately, our goal is to provide a comprehensive view of the 10 pc sample in a future paper in this series, once the *Gaia* DR2 results are available.

## 7. Conclusions

The RECONS astrometry/photometry program will continue at the CTIO/SMARTS 0.9 m, with two primary goals. First, several hundred of the nearest red dwarfs are being observed astrometrically to detect unseen companions in ~decade-long orbits, such as those shown in Figure 2, including a search for Jovian planets. Second, the same stars are being observed photometrically to measure their variability over long timescales to detect cyclic changes in brightness that mimic our Sun's solar cycle, as shown in Figures 3 and 4.

Now is an appropriate time to be circumspect about the accomplishments of the parallax program to date. Among the most important are:

1. Even after the YPC and *Hipparcos* parallax compendia were available, many of the Sun's neighbors had yet to be revealed. A total of 44 systems have been placed within the 10 pc sample via the RECONS program, including 41 red dwarf systems, 2 white dwarfs, and 1 brown dwarf. These 44 systems comprise 14% of all systems currently known within 10 pc of the Sun.
2. Many of the 14 close multiples among the 44 discoveries promise to yield highly accurate masses. Because of their proximity, detailed work on these systems will provide fundamental understanding of the characteristics of stars (and a few brown dwarfs) that depend on mass, the all-important parameter that determines nearly everything that occurs in the life of a star.
3. We predict that there are ~300 systems with stellar primaries within 10 pc, and that the current such sample is at least 90% complete.

[15] For many of the brown dwarfs, only relative $\pi_{\rm trig}$ have been computed, with no corrections to absolute $\pi_{\rm trig}$. Given the often large errors in their parallaxes, the correction is generally much smaller than the error, and the overall picture of the solar neighborhood census would be incomplete without these new members, so they are included here.

[16] As noted in Section 6.2, there are currently 38 systems containing only brown dwarfs known within 10 pc.

[17] Rankings here omit the brown dwarf systems UGPS 0722-0540, WIS 0855-0714, and WIS 1049-5319 AB.

Undoubtedly, some of the Sun's nearest neighbors have yet to be discovered, but great progress has been made over the past two decades. In addition to presenting here the critical parallaxes that place 44 new systems within 10 pc, we provide additional astrometric, photometric, and spectroscopic information that allows us to characterize these systems. With the list of nearby stars in hand, we are poised to continue the reconnaissance of the solar neighborhood in the search for planets orbiting these stars and, ultimately, life on those planets.

Colleagues at the Cerro Tololo Inter-American Observatory and the SMARTS Consortium have played integral parts in supporting the RECONS effort over two decades at CTIO, and we are indebted to all those at CTIO and SMARTS who have made this work possible. At CTIO, Alberto Miranda and Joselino Vasquez made a large number of observations at the 0.9 m over many years. Mountain operations have been supported by arguably the best observatory staff in the world, and we wish to thank Marco Bonati, Edgardo Cosgrove, Arturo Gomez, Manuel Hernandez, Rodrigo Hernandez, Peter Moore, Humberto Orrego, Esteban Parkes, David Rojas, Javier Rojas, Mauricio Rojas, Oscar Saa, Hernan Tirado, Ricardo Venegas, and so many others who have provided superb and enduring assistance with "The Best Telescope in the World" (TBTW), the CCD camera, and computer systems. Many students and colleagues have also been a part of this long-term work, and we are particularly indebted to Mark Boyd, Misty Brown, Edgardo Costa, Tiffany (Pewett) Clements, Cassy (Davison) Smith, Altonio Hosey, John Lurie, Rene Mendez, Hektor Monteiro, Leonardo Paredes, and R. Andrew Sevrinsky. We also thank Norbert Zacharias, who was instrumental in the URAT effort for which seven supporting parallaxes are included here.

The earliest phase of the RECONS astrometry/photometry program was supported by the NASA/NSF Nearby Star (NStars) Project through NASA Ames Research Center. The National Science Foundation has been consistently supportive of this effort under grants AST-0507711, AST-0908402, AST-1109445, AST-141206, and AST-1715551, while for several years the effort was also supported by NASA's *Space Interferometry Mission*.

This work has used data products from the Two Micron All Sky Survey, which is a joint project of the University of Massachusetts and the Infrared Processing and Analysis Center at the California Institute of Technology, funded by NASA and NSF. Information was collected from several additional large database efforts: the SIMBAD database and the VizieR catalogue access tool, operated at CDS, Strasbourg, France, NASA's Astrophysics Data System, the SuperCOSMOS Science Archive, prepared and hosted by the Wide Field Astronomy Unit, Institute for Astronomy, University of Edinburgh, which is funded by the UK Science and Technology Facilities Council, and the Washington Double Star Catalog maintained at the U.S. Naval Observatory.

## ORCID iDs

Wei-Chun Jao https://orcid.org/0000-0003-0193-2187
Jennifer G. Winters https://orcid.org/0000-0001-6031-9513
Adric R. Riedel https://orcid.org/0000-0003-1645-8596
Michele L. Silverstein https://orcid.org/0000-0003-2565-7909
John P. Subasavage https://orcid.org/0000-0001-5912-6191

## References

Andrei, A. H., Smart, R. L., Penna, J. L., et al. 2011, AJ, 141, 54
Bartlett, J. L., Lurie, J. C., Riedel, A., et al. 2017, AJ, 154, 151
Beichman, C., Gelino, C. R., Kirkpatrick, J. D., et al. 2014, ApJ, 783, 68
Benedict, G. F., Henry, T. J., Franz, O. G., et al. 2016, AJ, 152, 141
Benedict, G. F., McArthur, B., Nelan, E., et al. 1998, AJ, 116, 429
Benedict, G. F., McArthur, B., Chappell, D. W., et al. 1999, AJ, 118, 1086
Bessell, M. S. 1990, A&AS, 83, 357
Biller, B. A., Kasper, M., Close, L. M., Brandner, W., & Kellner, S. 2006, ApJL, 641, L141
Boffin, H. M. J., Pourbaix, D., Mužić, K., et al. 2014, A&A, 561, L4
Bonfils, X., Delfosse, X., Udry, S., et al. 2013, A&A, 549, A109
Boyd, M. R., Henry, T. J., Jao, W.-C., Subasavage, J. P., & Hambly, N. C. 2011, AJ, 142, 92
Burgasser, A. J., Gillon, M., Melis, C., et al. 2015, AJ, 149, 104
Burgasser, A. J., Tinney, C. G., Cushing, M. C., et al. 2008, ApJL, 689, L53
Clements, T. D., Henry, T. J., Hosey, A. D., et al. 2017, AJ, 154, 124
Costa, E., Méndez, R. A., Jao, W.-C., et al. 2005, AJ, 130, 337
Costa, E., Méndez, R. A., Jao, W.-C., et al. 2006, AJ, 132, 1234
Dahn, C. C., Harris, H. C., Subasavage, J. P., et al. 2017, AJ, 154, 147
Dahn, C. C., Harris, H. C., Vrba, F. J., et al. 2002, AJ, 124, 1170
Davison, C. L., White, R. J., Henry, T. J., et al. 2015, AJ, 149, 106
Davison, C. L., White, R. J., Jao, W.-C., et al. 2014, AJ, 147, 26
Deacon, N. R., Hambly, N. C., & Cooke, J. A. 2005a, A&A, 435, 363
Deacon, N. R., Hambly, N. C., Henry, T. J., et al. 2005b, AJ, 129, 409
Debes, J. H., & Kilic, M. 2010, AIP Conf. Ser. 1273, 17th European White Dwarf Workshop (Melville, New York: AIP), 488
Dieterich, S. B., Henry, T. J., Jao, W.-C., et al. 2014, AJ, 147, 94
Dittmann, J. A., Irwin, J. M., Charbonneau, D., & Berta-Thompson, Z. K. 2014, ApJ, 784, 156
Dupuy, T. J., & Liu, M. C. 2012, ApJS, 201, 19
ESA 1997, yCat, 1239, 0
Faherty, J. K., Burgasser, A. J., Walter, F. M., et al. 2012, ApJ, 752, 56
Faherty, J. K., Riedel, A. R., Cruz, K. L., et al. 2016, ApJS, 225, 10
Filippazzo, J. C., Rice, E. L., Faherty, J., et al. 2015, ApJ, 810, 158
Finch, C. T., & Zacharias, N. 2016, AJ, 151, 160
Finch, C. T., Zacharias, N., & Jao, W.-C. 2018, AJ, 155, 176
Finch, C. T., Zacharias, N., Subasavage, J. P., Henry, T. J., & Riedel, A. R. 2014, AJ, 148, 119
Gatewood, G., & Coban, L. 2009, AJ, 137, 402
Giammichele, N., Bergeron, P., & Dufour, P. 2012, ApJS, 199, 29
Gizis, J. E. 2002, ApJ, 575, 484
Gizis, J. E., Allers, K. N., Liu, M. C., et al. 2015, ApJ, 799, 203
Golimowski, D. A., Henry, T. J., Krist, J. E., et al. 2004, AJ, 128, 1733
Graham, J. A. 1982, PASP, 94, 244
Hambaryan, V., Staude, A., Schwope, A. D., et al. 2004, A&A, 415, 265
Hambly, N. C., Henry, T. J., Subasavage, J. P., Brown, M. A., & Jao, W.-C. 2004, AJ, 128, 437
Hartkopf, W. I., McAlister, H. A., & Franz, O. G. 1989, AJ, 98, 1014
Hawley, S. L., Gizis, J. E., & Reid, I. N. 1996, AJ, 112, 2799
Henry, T. J., Backman, D. E., Blackwell, J., Okimura, T., & Jue, S. 2003, Astrophysics and Space Science Library, Vol. 289, The Future of Small Telescopes In The New Millennium, Vol. III (Dordrecht: Kluwer), 111
Henry, T. J., Franz, O. G., Wasserman, L. H., et al. 1999, ApJ, 512, 864
Henry, T. J., Ianna, P. A., Kirkpatrick, J. D., & Jahreiss, H. 1997, AJ, 114, 388
Henry, T. J., Jao, W.-C., Subasavage, J. P., et al. 2006, AJ, 132, 2360
Henry, T. J., Kirkpatrick, J. D., & Simons, D. A. 1994, AJ, 108, 1437
Henry, T. J., Subasavage, J. P., Brown, M. A., et al. 2004, AJ, 128, 2460
Henry, T. J., Walkowicz, L. M., Barto, T. C., & Golimowski, D. A. 2002, AJ, 123, 2002
Herbig, G. H., & Moorhead, J. M. 1965, ApJ, 141, 649
Honeycutt, R. K. 1992, PASP, 104, 435
Hosey, A. D., Henry, T. J., Jao, W.-C., et al. 2015, AJ, 150, 6
Jao, W.-C., Henry, T. J., Beaulieu, T. D., & Subasavage, J. P. 2008, AJ, 136, 840
Jao, W.-C., Henry, T. J., Riedel, A. R., et al. 2016, ApJL, 832, L18
Jao, W.-C., Henry, T. J., Subasavage, J. P., et al. 2005, AJ, 129, 1954
Jao, W.-C., Henry, T. J., Subasavage, J. P., et al. 2011, AJ, 141, 117
Jao, W.-C., Henry, T. J., Subasavage, J. P., et al. 2014, AJ, 147, 21
Jao, W.-C., Henry, T. J., Winters, J. G., et al. 2017, AJ, 154, 191
Kendall, T. R., Jones, H. R. A., Pinfield, D. J., et al. 2007, MNRAS, 374, 445
Kirkpatrick, J. D., Schneider, A., Fajardo-Acosta, S., et al. 2014, ApJ, 783, 122
Landolt, A. U. 1992, AJ, 104, 372
Landolt, A. U. 2007, AJ, 133, 2502
Landolt, A. U. 2013, AJ, 146, 131

Leggett, S. K., Saumon, D., Marley, M. S., et al. 2012, ApJ, 748, 74
Leinert, C., Jahreiß, H., Woitas, J., et al. 2001, A&A, 367, 183
Lépine, S. 2008, AJ, 135, 2177
Lépine, S., Thorstensen, J. R., Shara, M. M., & Rich, R. M. 2009, AJ, 137, 4109
Luhman, K. L. 2013, ApJL, 767, L1
Luhman, K. L. 2014, ApJL, 786, L18
Luhman, K. L., & Esplin, T. L. 2016, AJ, 152, 78
Lurie, J. C., Henry, T. J., Jao, W.-C., et al. 2014, AJ, 148, 91
Luyten, W. J. 1979, in LHS Catalogue (2nd ed. ed. W. J. Luyten Minneapolis: Univ. Minnesota), 100
MacGregor, M. A., Weinberger, A. J., Wilner, D. J., Kowalski, A. F., & Cranmer, S. R. 2018, ApJL, 855, L2
Mamajek, E. E., Barenfeld, S. A., Ivanov, V. D., et al. 2015, ApJL, 800, L17
Mamajek, E. E., Bartlett, J. L., Seifahrt, A., et al. 2013, AJ, 146, 154
Marocco, F., Smart, R. L., Jones, H. R. A., et al. 2010, A&A, 524, A38
Montagnier, G., Ségransan, D., Beuzit, J.-L., et al. 2006, A&A, 460, L19
Nidever, D. L., Marcy, G. W., Butler, R. P., Fischer, D. A., & Vogt, S. S. 2002, ApJS, 141, 503
Pérez Garrido, A., Lodieu, N., Béjar, V. J. S., et al. 2014, A&A, 567, A6
Perryman, M. A. C., Lindegren, L., Kovalevsky, J., et al. 1997, A&A, 323, L49
Rajpurohit, A. S., Reylé, C., Allard, F., et al. 2013, A&A, 556, A15
Reid, I. N., Cruz, K. L., Kirkpatrick, J. D., et al. 2008, AJ, 136, 1290
Reid, I. N., Cruz, K. L., Laurie, S. P., et al. 2003, AJ, 125, 354
Reid, I. N., Hawley, S. L., & Gizis, J. E. 1995, AJ, 110, 1838
Riedel, A. R., Finch, C. T., Henry, T. J., et al. 2014, AJ, 147, 85
Riedel, A. R., Murphy, S. J., Henry, T. J., et al. 2011, AJ, 142, 104
Riedel, A. R., Subasavage, J. P., Finch, C. T., et al. 2010, AJ, 140, 897
Rodgers, A. W., & Eggen, O. J. 1974, PASP, 86, 742
Sahlmann, J., Lazorenko, P. F., Bouy, H., et al. 2016, MNRAS, 455, 357
Sahlmann, J., Lazorenko, P. F., Ségransan, D., et al. 2014, A&A, 565, A20
Schmidt, S. J., West, A. A., Burgasser, A. J., Bochanski, J. J., & Hawley, S. L. 2010, AJ, 139, 1045
Scholz, R.-D. 2014, A&A, 561, A113
Scholz, R.-D., Lo Curto, G., Méndez, R. A., et al. 2005, A&A, 439, 1127
Shkolnik, E. L., Anglada-Escudé, G., Liu, M. C., et al. 2012, ApJ, 758, 56
Smart, R. L., Tinney, C. G., Bucciarelli, B., et al. 2013, MNRAS, 433, 2054
Subasavage, J. P., Henry, T. J., Hambly, N. C., et al. 2005, AJ, 130, 1658
Subasavage, J. P., Jao, W.-C., Henry, T. J., et al. 2009, AJ, 137, 4547
Subasavage, J. P., Jao, W.-C., Henry, T. J., et al. 2017, AJ, 154, 32
Teegarden, B. J., Pravdo, S. H., Hicks, M., et al. 2003, ApJL, 589, L51
Tinney, C. G. 1996, MNRAS, 281, 644
Tinney, C. G., Faherty, J. K., Kirkpatrick, J. D., et al. 2014, ApJ, 796, 39
van Altena, W. F., Lee, J. T., & Hoffleit, D. 1995, yCat, 1174, 0
van Leeuwen, F. 2007, A&A, 474, 653
Vrba, F. J., Henden, A. A., Luginbuhl, C. B., et al. 2004, AJ, 127, 2948
Weinberger, A. J., Boss, A. P., Keiser, S. A., et al. 2016, AJ, 152, 24
Weis, E. W. 1986, AJ, 91, 626
Winters, J. G., Henry, T. J., Jao, W.-C., et al. 2011, AJ, 141, 21
Winters, J. G., Henry, T. J., Lurie, J. C., et al. 2015, AJ, 149, 5
Winters, J. G., Irwin, J., Newton, E. R., et al. 2018, AJ, 155, 125
Winters, J. G., Sevrinsky, R. A., Jao, W.-C., et al. 2017, AJ, 153, 14
Zapatero Osorio, M. R., Béjar, V. J. S., Miles-Páez, P. A., et al. 2014, A&A, 568, A6